

Notable Events

An overview of the Mw 9, 11 March 2011,
Tohoku earthquake

Ryota Hino

Tohoku University

Japan

Excerpt from the
Summary of the Bulletin of the International Seismological Centre:

Hino, R., An overview of the Mw 9, 11 March 2011, Tohoku earthquake, *Summ. Bull. Internatl. Seismol. Cent.*, January - June 2011, 48(1-6), pp. 100-132, Thatcham, United Kingdom, 2015, doi:10.5281/zenodo.998789.

8.2 An overview of the M_W 9, 11 March 2011, Tohoku earthquake

Ryota HINO
Tohoku University
Japan



8.2.1 Introduction

On March 11 2011, a great earthquake struck the eastern part of Japan. The origin time and hypocenter determined by the Japan Meteorological Agency (JMA) were 05:46:18.1 (UT) and 38.103N, 142.860E, 24 km. This hypocenter is located about 150 km offshore from northeastern Japan (Tohoku district) and beneath the landward side of the Japan Trench. Although the epicenter was not very close to land, very strong shaking with maximum ground accelerations reaching 1–2 g (Furumura *et al.*, 2011) caused serious damage in eastern Japan, including Tokyo about 400 km from the epicenter. A large tsunami devastated the coastal area. The tsunami inundated more than 5 km inland into the Sendai plain, and huge inundation heights and run-ups occurred along the rugged coast in the northern part (Mori *et al.*, 2011). The earthquake was named “the 2011 off the Pacific coast of Tohoku earthquake” by JMA, but here it will be denoted as “the Tohoku earthquake.”

The Centroid Moment Tensor (CMT) solution presented by JMA showed that this earthquake was a low-angle-thrust type, with strike, dip and slip angles of 193, 10 and 79 degrees respectively. This solution is consistent with thrust faulting along the boundary between the subducting Pacific plate and the overriding North American (or Amur) plate. The scalar moment was 4.2×10^{22} Nm (moment magnitude M_W 9.0). The Global CMT (Nettles *et al.*, 2011) and USGS W-phase moment tensor (Duputel *et al.*, 2011) solutions are almost the same as the JMA solution but with larger moment estimates, 5.3×10^{22} Nm (GCMT) and 4.5×10^{22} Nm (USGS). This earthquake is thus the largest instrumentally recorded earthquake in Japan, and the fourth largest in the world.

At the Japan Trench subduction zone, cold and old Pacific plate (110 Ma; Nakanishi and Winterer, 1998) is subducted with a convergence rate of 7 - 8.5 cm/year (e.g. Altamimi *et al.*, 2007). In terms of comparative subductology (Ruff and Kanamori, 1980) this subduction zone is different from the Chilean type, where large interplate earthquakes repeatedly occur. The seismic coupling coefficient here was estimated at less than 0.3, based on the recurrence history of interplate earthquakes along the Japan Trench (e.g. Kanamori, 1977; Seno, 1979; Peterson and Seno, 1984; Pacheco *et al.*, 1993).

The slip deficit rate along the subduction interface has been estimated from the deformation data provided by the nation-wide dense GPS network (e.g. Nishimura *et al.*, 2004; Suwa *et al.*, 2006; Hashimoto *et al.*, 2009; Loveless and Meade, 2010). The results indicate that the strength of interplate coupling is largely heterogeneous, having several peaks whose locations are well correlated with the rupture areas, estimated from analysis of historic seismograms, for the M 7–8 class Japanese earthquakes since about 1900 (Yamanaka and Kikuchi, 2004). Yamanaka and Kikuchi (2004) found a persistence of asperity locations throughout the earthquake cycle from these asperity maps and argued that large interplate earthquakes were repeating ruptures related to the asperities. Coincidence of the locked portions identi-

fied from geodetic observations with asperities for previous large earthquakes reinforced this idea. This suggested that aseismic slip takes place around the asperities and analysis of geodetic data showed that large-scale post-seismic slip after these large earthquakes occurred in 1978 (Ueda *et al.*, 2001), 1989 (Kawasaki *et al.*, 2001), 1992 (Kawasaki *et al.*, 1995) and 1994 (Heki *et al.*, 1997). All these afterslips released significant amounts of seismic moment around the asperities of the corresponding mainshocks.

Numerous small repeating earthquakes along the subduction interface have been observed on the outskirts of the asperities (Uchida *et al.*, 2003). These observations provided the basis for the assumption that large interplate earthquakes along the Japan Trench obey the characteristic earthquake model: the history of major earthquakes can be attributed to repeating failures of persistent asperities at quite regular intervals. The Earthquake Research Committee (ERC) in Japan have determined probabilities for large subduction earthquakes, based on historical records for more than 400 years, to make long-term forecasts of large earthquakes in the vicinity of Japan (<http://www.jishin.go.jp/main/index-e.htm>).

In the middle part of the main subduction zone, the Miyagi-oki region, where the Tohoku earthquake occurred, the ERC evaluated that a series of M 7 class earthquakes should recur at intervals of about 40 years. In this assessment, the earthquake in 1978 (M_W 7.4) was regarded as the typical type of earthquake in the region. However, Umino *et al.* (2006) discussed the diversity of the rupture patterns of earthquakes in the Miyagi-oki region, and considered that the 1978 earthquake was due to a compound rupture of smaller asperities that caused a series of M 7 class earthquakes in the 1930s. In 2005, an interplate earthquake of M_W 7.1 occurred in the region, and this was interpreted as a partial re-rupture of the asperity causing the anticipated M 7.5 class earthquake (Okada *et al.*, 2005) but leaving a substantial portion unbroken. Under these circumstances, the ERC evaluated that the forthcoming earthquake was imminent.

On the other hand, the ERC also indicated that an earthquake of $M > 8$ could occur as a consequence of synchronized failure of the Miyagi-oki asperity and an unknown asperity probably located on the trenchward side of the Miyagi-oki region, based on historical documents indicating a large earthquake associated with a significant tsunami in 1793. There were also several palaeoseismological studies indicating a sporadic occurrence of extraordinary earthquakes much larger than in the instrumental record. Tsunami deposits associated with the A.D. 869 Jogan and other similar earthquakes were identified on the Sendai plain and the broad areas to the south (Minoura *et al.*, 2001; Shishikura *et al.*, 2007; and Shishikura *et al.*, 2010). By modeling the inundation and subsidence, Sawai *et al.* (2012) estimated the Jogan earthquake as being of moment magnitude 8.4 or larger, with a fault rupture area 200 km long.

As explained so far, it had been believed that the state of interplate coupling was well understood along the Japan Trench subduction system. Therefore, the occurrence of the M 9 earthquake was surprising for most seismologists not only in Japan but also around the world. The most fundamental question raised by the Tohoku earthquake was how an M 9 earthquake could happen in a subduction zone characterized by the frequent recurrence of $M < 8$ earthquakes and broad aseismic slip. To address this question, it is important to characterize the rupture process of the Tohoku earthquake not only during the dynamic rupture of the mainshock but also in the periods before and after. This review examines results of extensive studies of the source of the Tohoku earthquake, of the plate boundary processes before the occurrence of the earthquake and also of the consequences of this great earthquake.

8.2.2 Rupture process of the Tohoku earthquake

Numerous source models of the Tohoku earthquake have been estimated based on seismic, geodetic, and tsunami observations made immediately after the rupture occurred. All the models, including those derived from joint inversion of different kinds of data sets (e.g. seismic + geodetic, geodetic + tsunami, seismic + geodetic + tsunami), estimated the total moment release in the range from 3 to 5×10^{22} Nm, remarkably consistent with one another, regardless of the data sources and methods, and also with the CMT solutions based on point source approximations. Nevertheless, the spatial distribution images presented for the coseismic slip show considerable diversity.

Numerous offshore observations made in and around the rupture region of the Tohoku earthquake have provided invaluable information constraining the rupture models for the earthquake. Tsunami waveform records without severe distortion due to non-linear effects near the coast showed several important features of the tsunami source (Hayashi *et al.*, 2011), as did the ocean-bottom pressure data obtained by the cabled systems (Maeda *et al.*, 2011) and the offline Bottom Pressure Recorders (BPR, Saito *et al.*, 2011). There were seven seafloor benchmarks of the GPS/acoustic seafloor geodetic survey within the rupture area, and observed large coseismic displacements, from 10 to 31 m horizontally (Sato *et al.*, 2011; Kido *et al.*, 2011), were solid evidence of large slip along the plate boundary fault. Y. Ito *et al.* (2011) reported very large horizontal displacements, greater than 50 m, at sites located close to the trench axis. The BPR deployed in the rupture area showed pressure changes associated with permanent vertical displacements (Y. Ito *et al.*, 2011; Inuma *et al.*, 2012; Hino *et al.*, 2013a) of the order of several metres. Fujiwara *et al.* (2011) indicated the change in topographic profile near the Japan Trench by comparing multibeam bathymetric data obtained before and after the mainshock. That analysis revealed that the displacements extended out as far as the Japan Trench, suggesting that the fault rupture reached the trench axis.

Among the various source models, tsunami inversions tended to resolve very large slip near the trench (Maeda *et al.*, 2011; Fujii *et al.*, 2011, Saito *et al.*, 2011; Gusman *et al.*, 2012; Hooper *et al.*, 2013; Satake *et al.*, 2013). The analyses of onshore geodetic data yielded models with a broad slip distribution spanning an area of 400 km \times 200 km (Ozawa *et al.*, 2011; Nishimura *et al.*, 2011; Inuma *et al.*, 2011; Pollitz *et al.*, 2011), but the slip model derived by including offshore deformation data mostly required a compact area of extremely large slip along the trench axis (T. Ito *et al.*, 2011; Loveless and Meade, 2011; Pollitz *et al.*, 2011, Romano *et al.*, 2012; Inuma *et al.*, 2012) except for the model presented by Hashimoto *et al.* (2012). Although some models derived from seismic waveform data showed a peak slip located close to the hypocenter, about 100 km away from the trench axis (Ammon *et al.*, 2011; Y. Yoshida *et al.*, 2011; Koketsu *et al.*, 2011; Yokota *et al.*, 2011), others with the largest slip nearer the trench have been presented (Ide *et al.*, 2011; Lay *et al.*, 2011a; Shao *et al.*, 2011; K. Yoshida *et al.*, 2011; Hayes, 2011; Lee *et al.*, 2011; Suzuki *et al.*, 2011; Yagi and Fukahata, 2011; Yue and Lay, 2011, 2013; Kubo and Kakehi, 2013).

Sources of coherent short-period seismic-wave radiation from the Tohoku earthquake were imaged by back-projection (BP) of the seismic waveform records obtained by seismic arrays located at local and at teleseismic distances (Honda *et al.*, 2011; Simons *et al.*, 2011; Wang and Mori, 2011a, b; Ishii 2011; Zhang *et al.*, 2011; Meng *et al.*, 2011; Koper *et al.*, 2011a, b; Yao *et al.*, 2012; Kiser and Ishii, 2012). All these studies reported that the origin locations of the high-frequency radiation derived from the BP

analyses were significantly different from the areas of very large slip. Sources of high-frequency seismic waves tended to be located along the deeper portions of coseismic slip but did not simply correlate with the locations of peak slip. Koper *et al.* (2011b) and Kiser and Ishii (2012) demonstrated that the locations of the imaged sources were strongly dependent on the frequencies used for the BP analysis and that the sources were located systematically on the more down-dip side for the shorter periods. Roten *et al.* (2012) applied BP methods to image the source radiating long-period Rayleigh waves, and found that the imaged Rayleigh wave sources were located significantly trenchward of the source locations of the short-period P-waves, supporting the interpretation of a frequency-dependent seismic-wave radiation.

Strong-motion records obtained by the local network were composed of three main identifiable wave packets as well as several less evident sub-events. Kurahashi and Irikura (2011, 2013), Asano and Iwata (2012) and Kumagai *et al.* (2013) tried to locate each strong-motion generation area (SMGA) for these strong-motion sub-events. All the SMGAs were located on the down-dip side of the patches of large coseismic slip determined from the inversions using the broad-band seismic data, geodetic data and tsunami data, but no SMGAs were located trenchward of the Tohoku earthquake hypocenter.

Bilek *et al.* (2012) and Ye *et al.* (2013) analyzed the dependence of source character on focal depth for other earthquakes along the Japan Trench and concluded that depth-varying source processes along the plate boundary fault in the area accounts for the frequency-depth relation observed for the seismic waves radiated from the Tohoku earthquake. Lay *et al.* (2012) identified similar variations in the frequency content of seismic waves in the records of the 2004 Sumatra-Andaman (M_W 9.1) and 2010 Chile (M_W 8.8) earthquakes and related the frequency dependence to the depth-varying frictional properties along the plate boundary fault. The heterogeneous radiation of different frequency content may therefore distort the slip distributions imaged by the seismic observations and account for the diversity of the source models.

As discussed earlier, the spatial variation of vertical deformation is expected to place strong constraints on the slip distribution. Although the tsunami wavefield basically reflects the vertical seafloor deformation, it could be distorted by several effects other than the pure vertical displacement associated with the fault motion: for example, additional tsunami generation caused by horizontal motion of a steep seafloor (Tanioka and Satake, 1996a; Hooper *et al.*, 2013), inelastic deformation of the sedimentary layer along the inner side of the trench (Tanioka and Seno, 2001) or a possible submarine landslide (Kawamura *et al.*, 2012; Grilli *et al.*, 2013). In this review, the slip model obtained by Iinuma *et al.* (2012) is used as the reference model to characterize the spatial pattern of coseismic slip associated with the Tohoku earthquake, because that study used the BPR seafloor-displacement data as well as all other available seafloor geodetic observations.

The largest coseismic slip was estimated to be larger than 50 m and the area of large slip was constrained to be 150 km \times 50 km: main-patch M in (Figure 8.14). There is another area with significant coseismic slip of more than 10 m extending out to the down-dip side of the hypocenter: sub-patch A. The location of sub-patch A corresponds to the location of the rupture area of normally expected Miyagi-oki earthquakes but the amount of slip during the Tohoku earthquake was much larger than the coseismic slip usually associated with the M 7.5 class earthquakes repeatedly occurring in the region. There is also another patch of significant coseismic slip to the south of the hypocenter: sub-patch B.

Slip distributions with the largest slip near the trench and two minor patches in the Miyagi-oki and

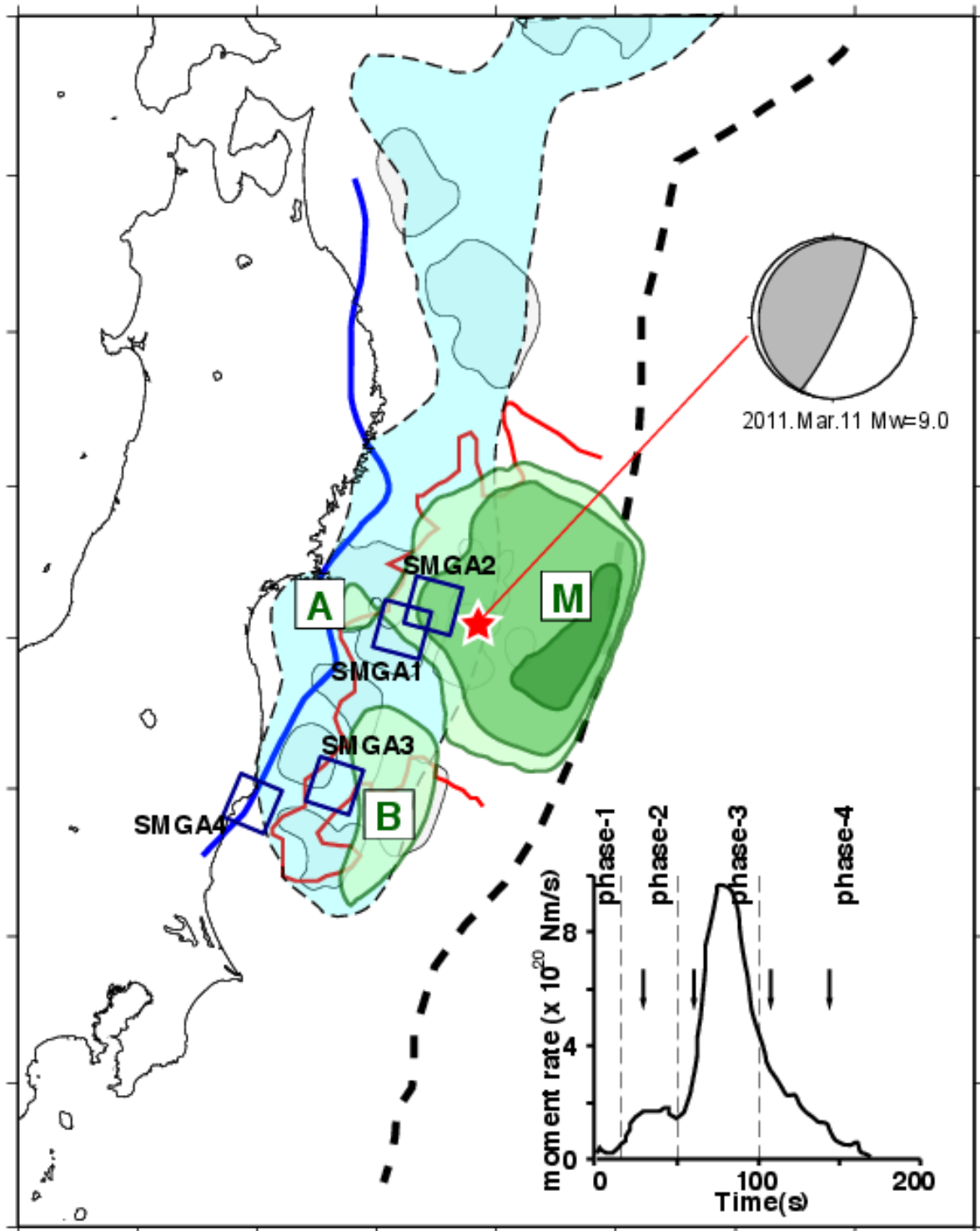


Figure 8.14: Source model (Inuma et al., 2012) and source-time function of the Tohoku earthquake (Suzuki et al., 2011). Areas are shaded light green for coseismic slip > 10m, green for slip > 20 m and dark green for slip > 50 m (Inuma et al., 2012). Squares represent SMGAs (Asano and Iwata, 2012). Rupture timing of each SMGA is shown beside the source-time function. The red line shows the outer limit of shallow interplate aftershock activity (Kato and Igarashi, 2012). The light blue area shows the zone strongly coupled before the mainshock (Hashimoto et al., 2009). Other shaded patches indicate rupture areas of previous $M < 8$ class interplate earthquakes (Yamanaka and Kikuchi, 2004). The blue line represents the down-dip limit of interplate seismicity (Igarashi et al., 2001), and the dashed black line represents the axis of the Japan Trench.

Fukushima-oki regions were also imaged in several of the studies, not just in geodetic data inversions (e.g. T. Ito *et al.*, 2011; Pollitz *et al.*, 2011, Romano *et al.*, 2012) but also in seismic and tsunami data investigations (Yagi and Fukahata, 2011; Yue and Lay, 2011, 2013; Fujii *et al.*, 2011).

Several models derived from the seismic data (Ide *et al.*, 2011; Lay *et al.*, 2011a, Shao *et al.* 2011; K. Yoshida *et al.*, 2011; Hayes, 2011; Suzuki *et al.*, 2011; Kubo and Kakehi, 2013) have a large slip area along the trench that extends much further to the south than in the reference model. However, these models did not have any moderate slip in the deeper portion corresponding to sub-patch B. Since the seafloor geodetic observations cannot be explained by the presence of significant fault slip near the trench in the south (Inuma *et al.*, 2012), the resolution in the dip direction for these slip models may have been poorer in the southern part of the rupture area of the Tohoku earthquake.

Spatiotemporal variation of coseismic slip along the plate boundary fault during the Tohoku earthquake was studied mostly using the analyses of broad-band seismograms recorded by local strong-motion networks, the global digital-seismographic network or from GPS data recorded at a high rate of sampling. Similarity among the moment-rate functions obtained in these studies is considerably high, indicating that temporal variation of the moment releasing rate is robustly constrained. Satake *et al.* (2013) attempted to reveal the space-time development of fault slip from tsunami observations, but that model differed mostly from the other seismic waveform inversions not only in the slip pattern but also in the moment rate function.

According to seismic data analyses, the length of significant moment release was about 160s. Duputel *et al.* (2013) considered that this earthquake was characterized by a temporally compact moment-rate function compared to other M -9 class earthquakes such as the 2004 Sumatra-Andaman, 1964 Alaska (M_W 9.2) and 1960 Chile (M_W 9.5) earthquakes. Okal (2013) also remarked, after analysis of ultra-long-period seismograms, that the Tohoku earthquake cannot be categorized along with slow-rupturing earthquakes.

From the source-time functions, the following four phases can be identified in common during the rupture process for the Tohoku earthquake (Figure 8.14):

Phase-1: an initial, very weak, energy radiation (0-10 s in lapse-time);

Phase-2: a moderate moment release with duration 40 seconds (10-50 s);

Phase-3: the largest moment release with duration 50 s, but up to 70 s (50 – 100 s);

Phase-4: a relatively long-lasting (> 60 s) moment release of moderate intensity (100s and later).

Ide *et al.* (2011) noted that the first three seconds of the Tohoku earthquake showed an emergent, relatively weak onset. Hoshiaba and Iwakiri (2011) mentioned not only the weakness of the initial seismic signals but also the strangeness of the frequency content. In particular, high frequencies early in the seismogram were more abundant than expected for an M 9 class earthquake and indistinguishable from that of the M -6 class foreshocks. Chu *et al.* (2011) examined the location, size, mechanism and the frequency content of the first four seconds of the earthquake and found that the Tohoku earthquake began as a small (M_W 4.9) thrust event. Uchide (2013) performed a multi-scale slip inversion analysis to show a complex rupture process during phase 1, in which the rupture direction changed, making the apparent rupture velocity very slow. Also, the M 7.3 foreshock occurring two days before in the vicinity of the mainshock hypocenter could have been a factor influencing the complex rupture propagation path

for the Tohoku mainshock,

After the small but complex initial rupture process around the hypocenter, the ruptured region started to grow rapidly through the next three phases (2 to 4). Although the observed seismic amplitudes were too small for analyses of local strong-motion records, the high-rate GPS data and the BP method gave good indications of the spatio-temporal development during these latter three phases.

The onsets of phase-2, phase-3 and phase-4 synchronized with the three major sub-events corresponding to the failure of SMGAs identified in the analysis off the local strong-motion data. The first two major slips occurred near the hypocenter, and a third occurred in the southern part of the rupture region (Kurahashi and Irikura, 2011, 2013; Asano and Iwata, 2012; Kumagai *et al.*, 2013). These three energetic subevents were also identified in the BP analysis (Zhang *et al.*, 2011).

One of the virtues of the BP method is that it tracks the source of high-frequency (HF) seismic signals during the rupture process. The BP studies using teleseismic data (Ishii, 2011; Wang and Mori, 2011a, b; Zhang *et al.*, 2011; Meng *et al.*, 2011; Yao *et al.*, 2012) consistently indicated that the center of the HF source moved quite slowly for approximately the first 90 s. Then the HF source center moved rapidly to the south and southwest. The timing of the sudden speed change roughly coincides with the onset of the phase-3 identified from the source-time function analyses.

Since the frequency content of the radiated seismic waves is dependent on the depth of the source, it may be difficult for the BP method to resolve the fault motion in the dip direction accompanying a change in depth. It is thus plausible that the very slow speed of rupture propagation estimated by the BP studies is indicative that the rupture propagation in the first 100 s occurred mostly in the fault-dip direction in the vicinity of the hypocenter. The rupture propagation process was also studied using the seismograms obtained at a dense seismic array located within a few hundred kilometres of the rupture area (Honda *et al.*, 2011; Nakahara *et al.*, 2011). These studies should give the trajectory of the HF sources at a higher resolution. Honda *et al.* (2011) showed bi-lateral rupture from the hypocenter in the up-dip and down-dip directions for about the first 40 s, whereas Nakahara *et al.* (2011) suggested predominantly down-dip rupture propagation in the same window.

The first moment release large enough to be detected by the high-rate GPS data started about 35 km west of the mainshock hypocenter at about 20 s lapse-time (Fukahata *et al.*, 2012). Because the location of this slip subevent is co-located with sub-patch A and its timing coincides well with phase-2 identified from the source-time function, it can be interpreted that phase-2 was the rupture of sub-patch A triggered by the rupture front propagating from the hypocenter. The first ruptured SMGA was also in the vicinity of sub-patch A (Asano and Iwata, 2012; Kurahashi and Irikura, 2013). The location of sub-patch A matches the source area that was expected for the next Miyagi-oki earthquake. However, the moment release from sub-patch A during the phase-2 was equivalent to M_W 8.5, which is much larger than the expected size of a Miyagi-oki earthquake (M 7.5).

It follows that phase-3 was the rupturing of the main-patch with an extremely large coseismic slip located along the trench releasing the largest moment, almost half the total. Yue and Lay (2011) reached the same conclusion. The BP analysis using seismic records in several different frequency bands (Ishii, 2011; Kiser and Ishii, 2012) showed that the radiation peak contemporaneous with the moment-rate peak was more prominent in the lower frequency bands, indicating predominant radiation from the large shallow

fault.

Kurahashi and Irikura (2013) located the SMGA broken at the onset of phase-3 at the down-dip edge of the main rupture area, whereas Asano and Iwata (2012) and Kumagai *et al.* (2013) placed the source of high-frequency radiation nearer the hypocenter in the main patch. The latter location could reasonably be explained if the radiation of short-period seismic signals reflected the actual onset of the main-patch rupture as suggested by Frankel (2013).

Based on results of the BP studies, the rupture process during phase-4 can be characterized by a rapid propagation towards the south, and with a moderate moment release from sub-patch B, located in the southern part of the ruptured region and elongated along the strike direction. In phase-4, high-frequency components were more dominant in the radiated intensities obtained by BP analysis (Ishii, 2011; Kiser and Ishii, 2012) than in phase-3, consistent with sub-patch B not lying along the trench. Multi-frequency BP analysis showed a revival of the low-frequency components during the final stage of the rupture history (lapse-time > 180 s), suggesting failure of the shallow fault (Kiser and Ishii, 2012). According to Kiser and Ishii (2012), this shallow rupture during the final stage could have acted as a tsunami source, although its contribution must have been quite minor because the amount of moment released after 180 s was considerably smaller in the source-time function.

8.2.3 Seismicity and slow slip along the plate boundary before the Tohoku earthquake

It is well known that the Tohoku earthquake was preceded by evident foreshock activity near the hypocenter of the mainshock. The region of this activity, shown in (Figure 8.15), was located almost near the up-dip extent of background interplate seismicity occurring before the Tohoku earthquake (Suzuki *et al.*, 2012; Ito *et al.*, 2013). An increase in seismicity of the region had started in February 2011, and a spatial expansion of this seismicity has been noted (Kato *et al.*, 2012; Suzuki *et al.*, 2012). The activity became significantly intense after the occurrence of the largest (M_W 7.3) foreshock on March 9, two days before the mainshock rupture. As shown by Marsan and Enescu (2012), the activity for the two days before the mainshock occurrence can be regarded as normal aftershock activity for an M_W 7.3 foreshock, as if nothing peculiar had happened.

It is common that aftershock activity after M -7 class interplate earthquakes is followed by evident afterslip in the Japan Trench region (e.g. Kawasaki *et al.*, 2001). Expansion of the aftershock regions have also been recognized (e.g. Tajima and Kennett, 2012), and these occurrences have been considered to be caused by aseismic slip and chain-reaction rupturing of small asperities along the plate boundary fault (Matsuzawa *et al.*, 2004). During the aftershock activity associated with the M_W 7.3 foreshock, clear expansion of this aftershock region (Ando and Imanishi, 2011; Kato *et al.*, 2012; Suzuki *et al.*, 2012) and evident crustal deformation was observable (Miyazaki *et al.*, 2011; Munekane, 2012; Ohta *et al.*, 2012), suggesting afterslip occurrence.

Kato *et al.* (2012) inferred, from a spatio-temporal evolution of tiny repeating earthquakes among the secondary aftershock activity for the largest foreshock, that aseismic afterslip propagated towards the hypocenter region of the mainshock. Ohta *et al.* (2012) showed that the afterslip occurred on the up-dip side of the M_W 7.3 foreshock hypocenter, whereas its coseismic rupture propagated in the down-dip

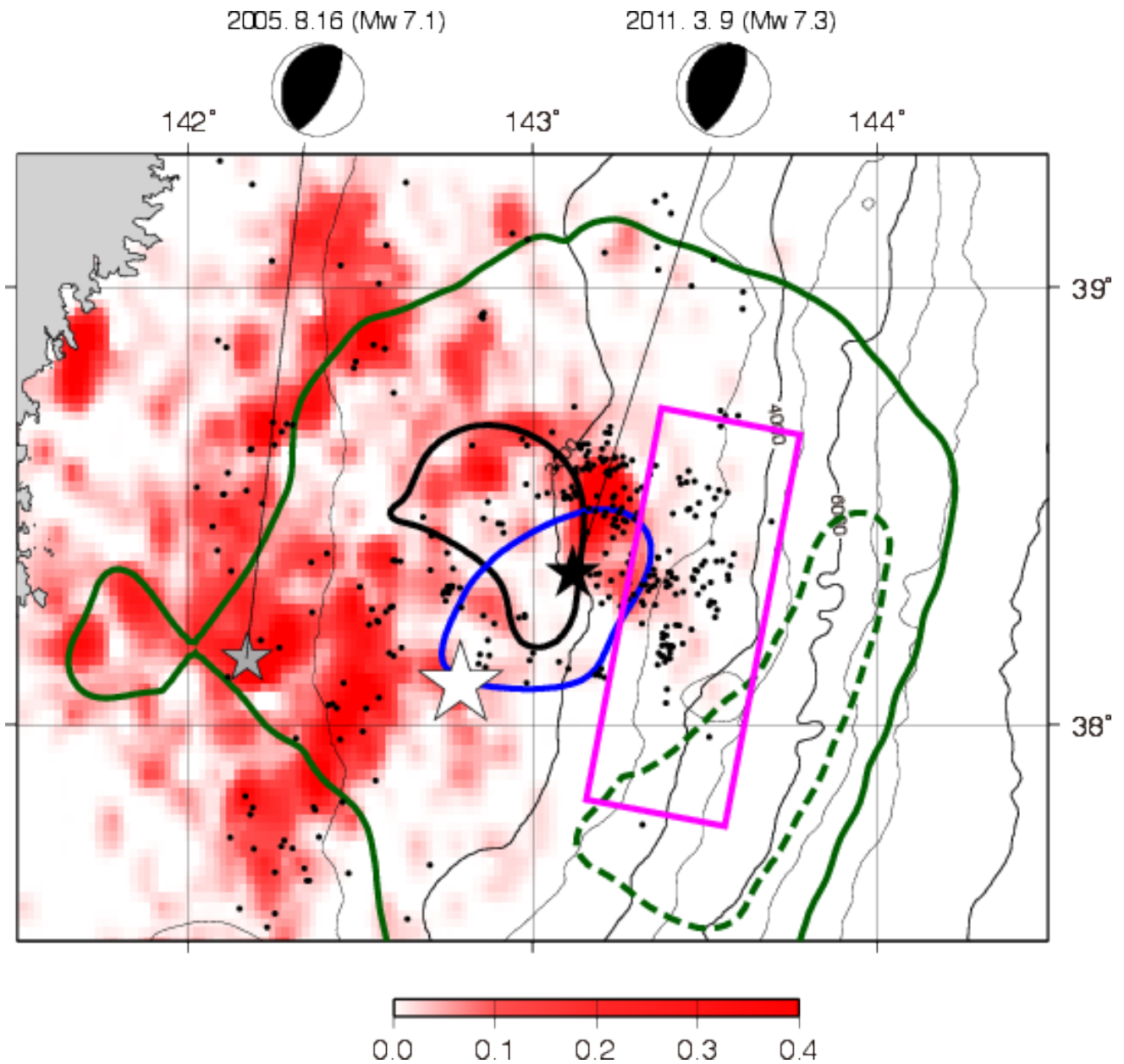


Figure 8.15: Seismicity and aseismic slip in the vicinity of the Tohoku earthquake before the occurrence of the mainshock. The reddish color scale shows a normalized density of epicenters in the background seismicity. Dots indicate epicenters of foreshocks, from the time of the largest foreshock (March 9) until the mainshock occurrence. The black contour represents the rupture region of the largest foreshock (slip > 0.5 m). The blue contour represents the afterslip region for the largest foreshock (March 9 to 11, slip > 0.3 m). The dark green solid and dashed lines represent contours of coseismic slip, at 10 m and 50 m respectively, for the Tohoku earthquake rupture. The pink rectangular outline indicates the source region of slow-slip, starting in February, 2011). Stars indicate epicenters of significant seismic events, including the previous most recent thrust earthquake in the Miyagi-oki region in 2005 (M_W 7.1).

direction (Ohta *et al.*, 2012; Gusman *et al.*, 2013). This afterslip released seismic moment equivalent to an M_W 6.8 event. The location of the afterslip region corresponds well with the aftershock distribution for the largest foreshock, and the mainshock hypocenter was located at the southwestern edge of this region. As usually observed for aftershock/afterslip phenomena in the Japan Trench subduction zone, there must have been some chain reaction for the continued activity, but what is most remarkable here is that one of the triggered small ruptures (M 5) grew into the great Tohoku earthquake through the rupture process as outlined in the previous section.

Ito *et al.* (2013) reported that another different type of aseismic slip event had occurred before this pre-imminent activity had started. That slip had occurred since the middle of February along the up-dip side of the afterslip zone associated with the March 9 foreshock. The region of this shallow slip was also associated with an increase in interplate seismicity, as pointed out by Kato *et al.* (2012), with the speculation that this shallow slow-slip had continued until the mainshock rupture occurred and then facilitated the large slip along the shallowest part of the plate boundary.

As explained so far, there were several indications of substantial aseismic slip in the vicinity of the Tohoku earthquake hypocenter, but there were no clear indications of any accelerated deformation occurring before the mainshock. Hirose (2011) and Hino *et al.* (2013b) inspected the continuous records from onshore tilt-meters and from offshore BPRs but could not identify any discernible changes in the deformation rate. Based on the detection level for these observations, Hino *et al.* (2013b) concluded that any accelerated aseismic slip related to nucleation for the mainshock rupture had to be smaller than for an M_W 6.2 event, if it occurred. Lack of any detectable precursory slip might be related to the nature of the initiation process of the Tohoku earthquake, but if the earthquake grew as the result of a cascading of very small earthquakes, its precursor must have been too small to be detected from the geodetic measurements of the earth surface.

In 1981, an M 7.1 earthquake occurred (Yamanaka and Kikuchi, 2004) almost in the same region, and although this must have been associated with similar afterslip and aftershock activity as in 2011 it did not trigger a great earthquake at that time. Sato *et al.* (2013) considered that the state of stress for the region was quite different in 1981 from that later in 2011, and that a series of $M < 7$ earthquakes had in the meantime loaded the region, priming it for rupture. Mitsui *et al.* (2012) suggested similarly.

Several studies have indicated that the Tohoku earthquake was preceded by precursory anomalies with a time scale of about 10 years, distinct from the shorter-term phenomena discussed so far. For the Miyagi-oki region, where large coseismic slip due to the mainshock and foreshock activity occurred, the b-value in the Gutenberg-Richter relationship was remarkably reduced before the Tohoku earthquake (Nanjo *et al.*, 2012), since about 2005. Tanaka (2012) reported on a tidal triggering of earthquakes, for several to ten years before the Tohoku earthquake, in almost the identical region to that where the b-value reduction was observed. Huang and Ding (2012) reported a reduced level of seismicity. Reduced seismicity has also been discussed by Katsumata (2011) but with the conclusion that the anomaly started much earlier, more than 20 years before the Tohoku earthquake.

Geodetic observations have led to proposals of an unzipping process for the plate boundary that had been tightly coupled in the earlier period. Suito *et al.* (2011) and Ozawa *et al.* (2012) showed that the durations and sizes of afterslip associated with the $M7$ class interplate earthquakes had tended to increase since 2005. The total moment of the aseismic slip for the nine years before the Tohoku earthquake was

equivalent to that of an M_W 7.7 earthquake, surpassing the total moment of the coseismic slip for the five largest earthquakes in the same period. Uchida and Matsuzawa (2013) noted that small but distinct increases in the slip rate in the period of about three years before the Tohoku earthquake near the area of large coseismic slip suggested there was pre-seismic unfastening of the locked area in the last stage of the earthquake cycle. Based on the synchronicity of these observed anomalies, it is likely that unfastening of the plate boundary fault accelerated aseismic slip and increased the shear stress along the fault.

8.2.4 Aftershock activity and postseismic deformation

Hirose *et al.* (2011) gave a general outline of the aftershock activity revealed by JMA monitoring. Soon after the occurrence of the Tohoku earthquake, extensive seismicity affected a broad area of Japanese territory, not only near the mainshock rupture region but also in inland areas ((Figure 8.16)). The number of aftershocks exceeded those following the 2004 Sumatra-Andaman earthquake and the 2010 Chile earthquake. In this section, the review will be concentrated on the seismicity on the Pacific Ocean side of Honshu, and the induced shallow crustal seismicity will be explained in a later section.

The area of the aftershock activity off Honshu was 500×100 km². In this region, three $M > 7$ earthquakes occurred within 40 minutes after the mainshock 05:46 origin-time. The first of these occurred at 06:08 to the north and the second at 06:15 to the south. These two large aftershocks were interplate events, judging from their thrust-type focal mechanisms, with magnitudes M_W 7.4 and M_W 7.7 respectively; the latter aftershock is the largest so far. At 06:25, an M_W 7.5 earthquake occurred beneath the outer rise of the Japan Trench, with a normal-type focal mechanism, indicating that this aftershock was an intraplate event within the shallow Pacific plate. The source models of these major aftershocks have also been estimated from onshore GPS data (Munekane, 2012). All these aftershocks were followed by their own sequences of (secondary) aftershocks.

Few interplate aftershocks with thrust focal mechanisms occurred within the large coseismic slip region, but several occurred instead in the surrounding regions (Asano *et al.*, 2011). Detailed focal-depth distributions obtained from event relocations using ocean bottom seismographic data (Suzuki *et al.*, 2012) demonstrated that the active interplate seismicity before the Tohoku mainshock had later completely ceased in the vicinity of the mainshock hypocenter. Tajima and Kennett (2011) pointed out that the aftershock area did not show significant expansion after the Tohoku earthquake and the two immediate large aftershocks, whereas all previous major interplate earthquakes, including the largest foreshock on March 9, had had a significant enlargement of aftershock area associated with them. To the north of the mainshock rupture, interplate moment release in previous large earthquakes (e.g. M_W 7.7 in 1994) and the subsequent slow slip may have prevented the propagation of slip along the plate boundary fault (Kosuga and Watanabe, 2011). Kubo *et al.* (2013) examined the coseismic slip model for the largest aftershock and found that its rupture expansion was inhibited by the existence of the Philippine Sea plate, which is subducted from the south between the inland plate and the Pacific plate.

Low seismicity along the rupture region of the mainshock has been reported for the aftershock activity following several large earthquakes (e.g. Scholz, 2002; Hino *et al.*, 2000; Hino *et al.*, 2006). Kato and Igarashi (2012) pointed out that there was a clear border for the low in-plane seismicity and suggested that this border could be considered to be the outer rim of the high-slip zone during the Tohoku earth-

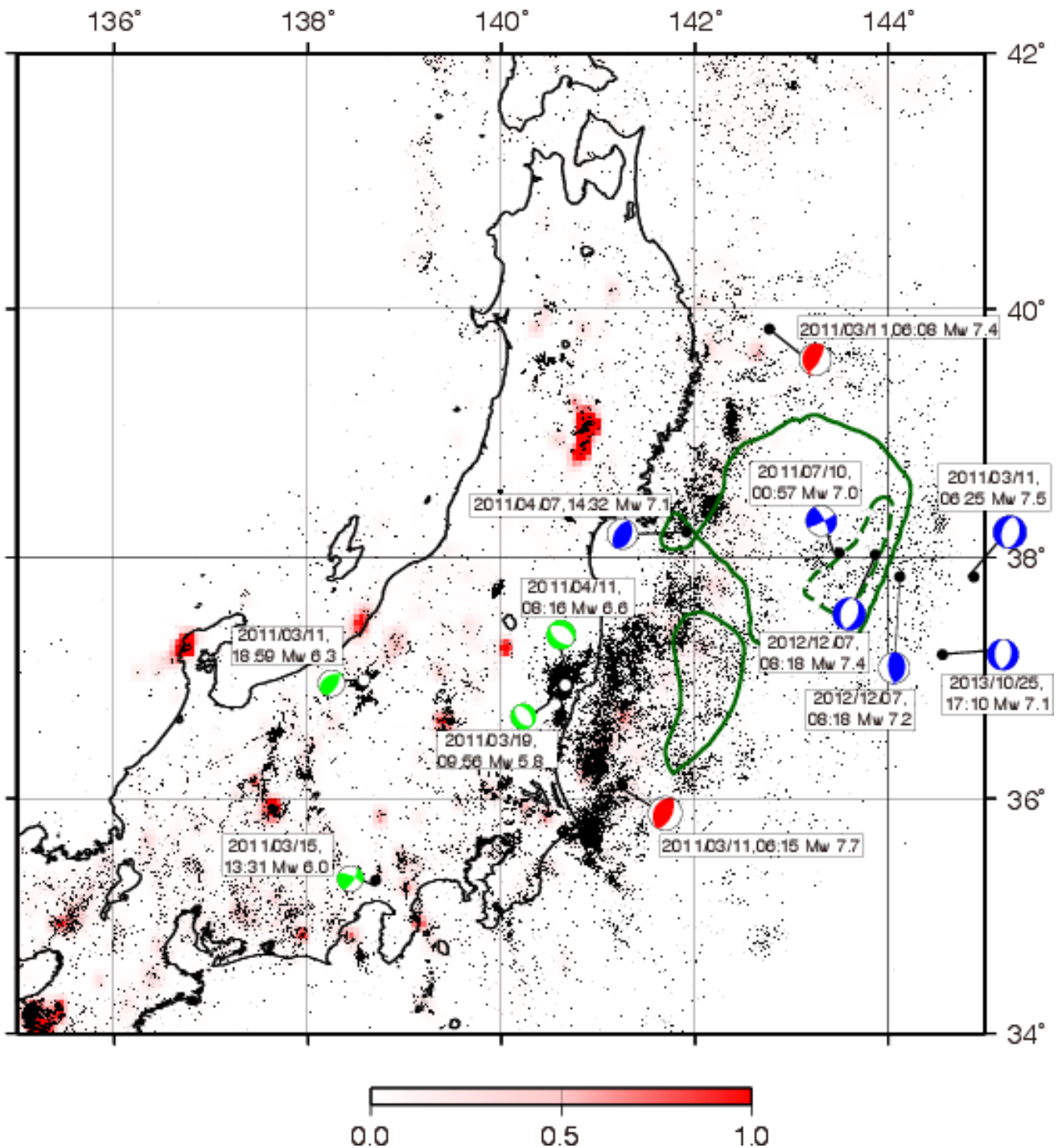


Figure 8.16: Aftershock epicenters and remote induced seismicity from March 11 to December 31, 2011. Epicenters are from the JMA catalog. Focal mechanism solutions for notable recent earthquakes are those determined by F-net, except for the intraslab doublet on December 7, 2011. For the doublet, CMT solutions provided by JMA (2013) are shown. Red, blue and green solutions represent interplate, intraplate in the Pacific plate, and shallow crustal earthquakes, respectively. The reddish color scale shows a normalized density of background seismicity.

quake. Outside this border, active aftershock seismicity was probably caused by the stress concentration due to a large contrast in fault slip.

After the intra-Pacific-plate earthquake beneath the outer rise of the Japan Trench at 06:25 on March 11 (M_W 7.5), all the subsequent aftershocks with $M > 7$ occurred within the Pacific plate. There are several previous examples where shallow normal-faulting earthquakes in the outer-rise trench regions have been triggered by large megathrust earthquakes (Lay *et al.*, 2011b). In the Japan Trench subduction zone, the large M_W 8.3 normal faulting earthquake in 1933 is considered to have been triggered by the shallow thrust-faulting earthquake in 1896. Hypocenters in the 2011 normal-faulting aftershock region were not distributed along a simple plane corresponding to the rupture plane of the M_W 7.5 aftershock, but were instead located along several parallel planes (Obana *et al.*, 2012), suggesting that several shallow normal faults in the outer rise region were all activated at about the same time by the Tohoku earthquake.

In the outer region of the Japan Trench, intraplate seismicity formed a double-planed structure: an upper plane in the lower crust and uppermost mantle of the oceanic lithosphere, and a lower plane located about 30 km beneath it. The focal mechanisms of the upper plane earthquakes were mostly of the normal-faulting type with trench-normal T-axes, whereas those in the lower plane were of the reverse-faulting type with trench-normal P-axes, (Gamage *et al.*, 2009; Hino *et al.*, 2009). These observations indicated that the upper and lower planes were under tensional and compressional stress respectively, caused by downward bending of the oceanic slab. Obana *et al.* (2012) reported that normal-faulting earthquakes were recognized down to 40 km in depth, well below the upper-plane seismicity, and suggested that the bending stress increased in response to the Tohoku earthquake.

A large, shallow, normal-faulting earthquake of M_W 7.1 occurred on October 25, 2013, about 100 km south-southwest of the M_W 7.5 aftershock, showing that the enhancement of the bending stress has lasted for quite some time along a broad region of the outer trench slope. Nearer the trench axis region, a pair of large earthquakes successively occurred within 14 s on December 7, 2012. This doublet began with an M_W 7.2 thrust-faulting event 50–70 km deep in the Pacific plate and was followed by a shallower M_W 7.1–7.2 normal-faulting event 10–30 km deep (Lay *et al.*, 2013). The occurrence of this doublet can also be explained as due to enhancement of the bending stress near the trench caused by the Tohoku mainshock (Harada *et al.*, 2013; Obana *et al.*, 2014).

Normal-faulting seismicity was also observed generally occurring within the subducted Pacific slab, mostly beneath the large coseismic slip region of the Tohoku mainshock (Asano *et al.*, 2011). These normal-faulting aftershocks near the trench and in the outer-rise region occurred mainly in the up-dip portion of the slab, where a tensional stress change can be attributed to the thrust-faulting of the mainshock. On July 10, 2011, an intraslab earthquake (M_W 7.1) occurred near the hypocenter of the Tohoku mainshock. This aftershock had a strike-slip mechanism with the T-axis oriented in the dip direction of the slab. The secondary aftershocks of this aftershock formed two orthogonal planes, conforming to the nodal planes for the focal mechanism of that large July 10 aftershock. That aftershock was interpreted as due to the reactivation of pre-existing weak faults, possibly related to irregularities in the formation process of the oceanic lithosphere (Obana *et al.*, 2013). Stress-tensor inversions from focal mechanisms of these shallow intraslab earthquakes revealed that the minimum principal stress axis was oriented in the plate-convergent direction in the postseismic period (Hasegawa *et al.*, 2012). This change in stress regime in the slab is consistent with mainshock-slip models having an extremely large

coseismic slip near the trench.

In contrast, an increase in the compressional stress in the slab is expected near the down-dip end of the high-slip region of the Tohoku earthquake. Indeed, an earthquake (M_W 7.1) occurred in the Pacific slab on 7 April. This aftershock occurred within the upper plane of the double-planed deep seismic zone beneath the northeastern Japan (Hasegawa *et al.*, 1978) and its down-dip compressional focal mechanism is consistent with those of the upper-plane events in the background seismicity. However, the M_W 7.1 earthquake rupture extended below the deeper limit of the usual distribution for the upper-plane seismicity and it was suggested that the down-dip compressional stress was largely intensified (Ohta *et al.*, 2011).

In the hanging wall, several small normal-faulting earthquakes occurred after the Tohoku earthquake. The T-axis directions of these aftershocks were diverse (Asano *et al.*, 2011). Shallow normal-faulting events were also identified in the aftershock activity following the 1994 Sanriku earthquake (Hino *et al.*, 2000), located to the north of the rupture region of the Tohoku earthquake. These shallow aftershocks occurred as a result of stress changes caused by the mainshock. A larger size of coseismic slip, in terms of area and slip amount, resulted in more intensive activity in the broader region in 2011 than it had in 1994.

Hasegawa *et al.* (2011) and Chiba *et al.* (2012) evaluated the stress field in the hanging wall using stress tensor inversions from focal mechanism solutions. Because there had been seismicity in the hanging wall before the Tohoku earthquake, the difference in the stress field before and after this great interplate earthquake could be estimated. From the comparison, it turned out that the maximum compressive-stress axis, having a usual direction aligned with the plate convergence, rotated by 30 to 35 degrees during the rupture of the Tohoku earthquake. This large coseismic rotation of the stress axis was interpreted as being caused by the complete stress release associated with the Tohoku earthquake. Hardebeck (2012) reported that the stress axes rotated rapidly back again to the usual orientation in the months following the Tohoku earthquake. It was considered that this rapid postseismic rotation was possible because the near-complete stress drop left very little background stress at the beginning of the postseismic reloading. Yagi and Fukahata (2011) also pointed out, based on their analysis of the mainshock rupture process, that the Tohoku earthquake released almost all the accumulated shear stress along the fault.

The Tohoku earthquake was followed by a large postseismic deformation across a broad region of eastern Japan. In early studies characterizing the afterslip, it was usually assumed that the observed postseismic deformation had been caused by slip along the plate boundary fault. Ozawa *et al.* (2011) showed significant expansion of the afterslip area extending out of the down-dip side of the coseismic rupture and also a fast moment release equivalent to M_W 8.3 within the two weeks after the mainshock occurrence. Ozawa *et al.* (2012) pointed out that afterslip along the deep plate interface continued for half a year but that the total slip tended to be smaller on the down-dip side of the Miyagi-oki region where the peak of coseismic slip was imaged.

A detailed account of postseismic slip in the earliest stage has been given by Munekane (2012). Within the 10-minute period between the mainshock and M_W 7.3 interplate aftershock to the north, afterslip propagated into the adjacent region to the north and down-dip of the mainshock rupture region, releasing seismic moment equivalent to an event of M_W 7.1. In the four-hour period after the largest aftershock (M_W 7.6) to the south of the mainshock, the slip propagated into the regions up-dip and down-dip of

the initial slip area, with a moment release equivalent to M_W 7.8. Johnson *et al.* (2012) and Fukuda *et al.* (2013) assessed the frictional properties of the plate boundary fault, based on the spatio-temporal evolution of the post-Tohoku earthquake slip, focusing on the complementary nature of the coseismic and postseismic slips and the moment-rate release dependency.

Although the afterslip estimates in these studies were based on the onshore GPS data, offshore observations of postseismic motion are required to describe the afterslip distribution precisely. The postseismic deformation patterns reported by Japan Coast Guard (2012) and Japan Coast Guard and Tohoku University (2013) were significantly different from the one estimated from the onshore observations. The most striking features in the offshore GPS observations were landward motions recorded in the Miyagi-oki region with the largest coseismic slip during the mainshock and subsidence across a broad region. It is unlikely that these features can be explained by afterslip alone and an alternative mechanism must also have been involved in the post-Tohoku earthquake deformation.

The most plausible mechanism controlling postseismic deformation other than afterslip on the fault is viscoelastic relaxation of the earthquake-induced stress (e.g. Wang *et al.* (2012). Diao *et al.* (2014) estimated that the effect of the viscoelastic relaxation within this initial stage only played a secondary role. However, the offshore postseismic displacements, completely opposite to those in the onshore region, indicated the importance of viscoelastic relaxation in interpreting the crustal deformation after the large stress perturbation induced by the Tohoku earthquake. Iinuma *et al.* (2014) computed the postseismic deformation observed at onshore and offshore sites as a combination of effects of afterslip and viscoelastic deformation.

Because of poor knowledge of the rheological structure in the subduction system, it is still difficult to obtain a reliable afterslip distribution along the plate interface. Nevertheless, the following three features were robustly obtained: 1) significant slip occurred on the deep extension of the mainshock rupture zone, 2) the amount of afterslip was minimal in the large coseismic slip area located in the Miyagi-oki region, and 3) occurrence of afterslip near the trench in the southern area, near the up-dip side of sub-patch B.

Heki and Mitsui (2013) pointed out that finite viscosity of the asthenosphere could have caused acceleration of the subducting motion of the Pacific plate due to a postseismic adjustment of the force balance acting on the slab, and argued that acceleration of the slab motion and rapid restoration of interplate coupling may have accounted for the landward postseismic motion in the Miyagi-oki region.

On the other hand, the activity of small repeating earthquakes along the plate boundary seems to have been driven solely by fault slip in a region free from the complexity of postseismic deformation. Uchida and Matsuzawa (2013) indicated an evident increase of the repeating earthquake activity in the regions surrounding the mainshock rupture zone, not only on the deeper side but also in the shallower part where the occurrence of significant afterslip was revealed by Iinuma *et al.* (2014). The slip rate estimated from the repeating earthquakes showed a more abrupt increase after the mainshock in the region closer to the source, suggesting outward propagation of afterslip from the rupture area.

8.2.5 Shallow crustal seismicity induced by the Tohoku earthquake

Shallow crustal seismicity was increased immediately after the Tohoku mainshock over a broad region of eastern Japan including several remote regions (Hirose *et al.*, 2011). The induced seismicity in remote

regions included several $M > 6$ earthquakes that caused severe damage around their focal regions. Okada *et al.* (2011), Toda *et al.* (2011a) and Ishibe *et al.* (2011) reported that static stress transfer after the Tohoku earthquake was responsible for these phenomena. Okada *et al.* (2011) pointed out that the estimated positive Coulomb stress change was mainly due to the reduction of normal stress on the fault planes. Toda and Stein (2013) warned that the probability of a large earthquake occurrence near the Tokyo metropolitan area had increased two-and-a-half times above that estimated before the Tohoku earthquake struck, due to the static stress change applied to the region following the Tohoku earthquake.

Kato *et al.* (2011) examined the coseismic static stress change in the coastal region of southern Tohoku where an M_W 5.8 normal-faulting earthquake occurred on March 19 and concluded that the earthquake occurred in response to an abrupt flip of the stress field from the pre-seismic trench-normal horizontal compression (e.g. Terakawa and Matsu'ura, 2010) to east-west extension after the Tohoku mainshock. Yoshida *et al.* (2012) showed that the directions of principal stress axes inferred from post-Tohoku focal mechanisms at several places in eastern Japan were consistent with those resulting from stress perturbations due to the Tohoku earthquake. Because the magnitudes of the applied stress changes were estimated at less than 1 MPa, a low differential stress before the Tohoku earthquake is a necessary condition at these locations.

On the other hand, Toda *et al.* (2011b) demonstrated that seismicity can occur in the nominal stress shadow of a mainshock as long as small geometrically diverse active faults exist. Imanishi *et al.* (2012) found that the pre-Tohoku earthquake stress field in the southern Tohoku region, for which the coseismic flip of the stress field was supposed by Kato *et al.* (2011), was a normal-faulting stress regime in contrast to the predominant reverse-faulting regime in northeastern Japan. In that southern region, small-scale heterogeneity had already existed and fractures in the normal-faulting region were reactivated by the enhancement of trench-normal extension after the Tohoku earthquake, causing intense shallow crustal seismicity. These arguments emphasize the importance of small-scale heterogeneity of the pre-mainshock stress state when interpreting an apparent coseismic change in the dominant focal mechanisms. Coseismic change in pore-fluid pressure can be another factor increasing the seismicity of the shallow crust in inland regions. Terakawa *et al.* (2013) argue that several induced earthquakes from unfavorably oriented faults after the Tohoku earthquake turn to optimally oriented faults with the ambient fluid pressure.

Among the induced inland seismicity, the largest earthquake of M_W 6.6 occurred in the southern part of the coastal region on 11 April 2011 (the Fukushima-ken-Hamadori earthquake or Iwaki earthquake) and ruptured two previously mapped faults. It was supposed that previous activity on these faults was related to earlier great interplate earthquakes like the Tohoku earthquake, assuming that the large ruptures along these faults had been induced exclusively by similar interplate earthquakes. A paleoseismic trench (Toda and Tsutsumi, 2013) across one of these faults exposed evidence for the penultimate earthquake that occurred about 15,000 years ago but there was no evidence that the fault ruptured during or immediately after the A.D. 869 Jogan earthquake.

There have been several reports of the induced seismicity being caused by dynamic stress change (e.g. Yukutake *et al.*, 2011; Kato *et al.*, 2013). Miyazawa (2011) showed that early post-seismic events triggered by the Tohoku earthquake propagated systematically across Japan. The propagation speed of the front of seismicity was consistent with that of the large amplitude surface waves. It was also found that small amplitude P-waves from the Tohoku earthquake could trigger non-volcanic tremor along the

Nankai Trough subduction zone (Miyazawa, 2012).

8.2.6 Discussion

Coseismic phenomena associated with the Tohoku earthquake have provided important clues to resolve the question of how a M -9 class earthquake could occur in the Japan Trench subduction margin, normally characterized by the frequent recurrence of $M < 8$ earthquakes and broad aseismic slip. In the most trenchward zone where the coseismic slip was the largest, the background seismicity was especially low. In contrast, the deeper portion of the plate boundary, where M 7.5 earthquakes have repeatedly occurred, slipped by about a third of that in the trench region. Taking the 1978 earthquake as a representative example, past earthquakes resulted in a dislocation of about 2 m due to coseismic activity and afterslip, and the total amount of this slip accounts for about two thirds of the slip deficit that accumulated within the recurrence interval (40 years) at a convergence rate of 0.08 m/year. The proportion of the coseismic slip between the deep seismogenic zone and the trenchward zone (1:3) is reasonably explained if the trenchward aseismic zone had been fully coupled and if the Tohoku earthquake released the strain accumulated since the previous M 9 earthquake, which may have occurred more than 600 years ago.

From this inference, it is emphasized that restoration of the history of large events associated with slip near the trench is indispensable to understanding the entire process of deformation, strain accumulation and release, caused by the subduction of the Pacific plate at the Japan Trench. Even though tsunami deposits along the coast are important records of past gigantic tsunami, the area of inundation of coastal regions such as the Sendai plain is not sensitive to the amount of slip near the trench (Sawai *et al.*, 2012). Besides onshore geologic investigations, systematic offshore studies for records of past large slip along the shallow subduction thrust zone are also required. Kodaira *et al.* (2012) reported that large-scale deformation structures near the trench axis have been developed by not only the large slip associated with the Tohoku earthquake but also in similar events repeatedly occurring in the past. These deformation structures could be indications of slip breaking through to the trench. A detail survey of submarine geologic structures should help to find where large earthquakes occurred previously. Strasser *et al.* (2013) studied sediment cores retrieved from the trench region and found evidence of large-scale slumping triggered by slip towards the trench. Analyses of sediment cores, which may provide direct or indirect indications of sudden large slips, may shed light on the recurrence history of the large-scale shallow faulting events.

Afterslip distribution provides key information on frictional properties along the plate boundary fault. Numerous efforts have been made to explain the rupture process of the Tohoku earthquake (e.g. Kato and Yoshida, 2011; Mitsui *et al.*, 2012), and the earthquake cycle along the Japan Trench, particularly the coexistence of regular M 8 and sporadic M 9 earthquakes (e.g. Hori and Miyazaki, 2011; Shibazaki *et al.*, 2011; Ide and Aochi, 2013). In all these models, frictional properties were important but not well constrained by the observations. As explained in the previous section, monitoring the activity of small repeating earthquakes puts strong constraints on the afterslip distributions. Along the Japan Trench, seafloor geodetic observations have been reinforced (Kido *et al.*, 2012) to understand better the postseismic deformation near the large coseismic slip area for the Tohoku earthquake.

On the other hand, it is also important to determine from the geodetic observations the extent of

deformation due to viscoelastic relaxation. To this end, realistic modeling of the rheological structure is critically important and this might also be resolved by the geodetic observations of the post-Tohoku earthquake deformation. Takahashi (2011) and Ohzono *et al.* (2012) reported strain changes as large as 45×10^{-6} in the onshore Tohoku region and pointed out that there were significant irregularities in the strain field induced by the Tohoku earthquake. These irregularities reflect spatial heterogeneity of the rheological structure and correlate with the spatial patterns of strain concentration observed before the mainshock. By including the spatio-temporal variation of postseismic deformation in the modeling, the rheological structure beneath the Japan Trench subduction zone could be resolved.

Stress changes associated with the Tohoku earthquake have provided invaluable opportunities to understand the stress field in the crust. Because the Tohoku earthquake was considered to release completely the shear stress accumulated along the plate boundary fault (Hasegawa *et al.*, 2011; Yagi and Fukahata, 2011), the level of differential stress on the plate interface can be estimated from the stress drop for this earthquake, 10 MPa. As the stress field after the earthquake can be expressed as the sum of the pre-seismic field and the coseismic static-stress change, Hasegawa *et al.* (2012) estimated the magnitude of the differential stress to be 10 MPa in the hanging wall of the large coseismic slip region.

The estimated magnitude of deviatoric stress implies that the strength of the plate boundary fault was weak, as it was also for faults in the hanging wall. Similarly, the significant difference in the stress field in the inland crust before and after the Tohoku earthquake (Kato *et al.*, 2011; Yoshida *et al.*, 2012) may also indicate that the shallow crustal faults were extremely weak, because the magnitude of the static stress change must have been very small (< 1 MPa) in the areas of significant changes in focal mechanisms. However, careful re-assessments regarding these proposals may be required since the observed stress changes may be merely apparent, caused by small-scale spatial variations of the stress field in the vicinity of the induced seismicity (Imanishi *et al.*, 2012).

As most of the tsunami inversion results indicated, the large coseismic slip near the central Japan Trench generally accounted for the size of the tsunami associated with the Tohoku earthquake. However, these models were unable to reproduce the magnitude of the observed tsunami run-up along the coastal region north of 39°N , whereas misfits of the model-predicted values were very small for the other observations, the run-up or inundation in the south and the offshore tsunami waveforms (MacInnes *et al.*, 2013). It was suspected that there must have been an additional source of tsunamigenic energy responsible for the large run-up in the northern coastal region. As reviewed by Satake and Fujii (2014), the observed coastal tsunami height distribution seemed to require a delayed tsunami source in the north of the earthquake source region. For example, the tsunami source model of Satake *et al.* (2013) with a delay (of more than three minutes after the mainshock initiation) in the rupture of the shallowest part of the fault near the northern Japan Trench, where no significant slips had been imaged by the previous studies, overcame the anomalies. However, the moment-rate time-series and source-time function of that time-dependent tsunami source model were not consistent with the other results derived from the seismic observations.

Since the delayed tsunami source was located near the source region of the 1896 tsunami earthquake (Tanioka and Satake, 1996b), the real nature of this enhanced tsunami source needs to be known. The size of delayed source was equivalent to a fault slip of more than 10 m, much larger than the slip deficit accumulated during about 100 years, even assuming 100% coupling.

8.2.7 Summary

The Tohoku earthquake has become an unprecedentedly well-described $M=9$ earthquake through a diversity of observations, including seismic and tsunami waveforms recorded in the far-field using global networks and large-scale arrays in North America and Europe, and non-clipped data in the near-field provided by overwhelmingly dense networks deployed in Japan. Emerging observation technology, such as high-rate GPS data collection as well as offshore tsunami, earthquake and geodetic observations, has helped to constrain the unique character of the Tohoku earthquake, with an extremely large slip along the shallowest portion of the subduction plate boundary. The frequency content of the radiated seismic energy was found to be strongly dependent on the depth, with higher frequencies predominantly from the deeper region in contrast to lower frequencies from the shallow fault region that was characterized by large slip.

Although the rupture spanned a large region beneath the landward slope of the Japan Trench, there was a more compact patch near the hypocenter where most of the moment release was concentrated. The earthquake completely released the shear stress accumulated along the plate boundary fault for more than a hundred years and caused a remarkable increase in seismicity across a broader region of Japan. Several lines of evidence have indicated that the Tohoku earthquake was preceded by an unloosening of the interplate coupling over an interval of about ten years, but no evident acceleration was observed to be related to the nucleation of a great earthquake except for foreshock activity associated with aseismic slip near the hypocenter.

Extensive afterslip along the down-dip extension of coseismic fault slip accounted for the postseismic deformation observed onshore, but the deformation included a substantial contribution from viscoelastic relaxation after the large coseismic slip, especially in the offshore area. The large impact of the Tohoku earthquake on the stress-strain field of the subduction zone has provided an invaluable opportunity to understand various aspects of the rheological characteristics of the lithosphere: absolute magnitude of crustal stress, fault strength, structure of viscosity, and so on. Efforts to monitor seismicity and crustal deformation will continue to be increasingly important.

8.2.8 Acknowledgements

The author wishes to thank Akira Hasegawa, Toru Matsuzawa, and Shinji Toda for discussions regarding the generation processes of the Tohoku-oki earthquake and its consequences. I would like to express respect for all the institutions around the world running seismological, geodetic and tsunami observation networks, providing invaluable data. In particular, outstanding contributions of the local networks operated by Japan Meteorological Agency (JMA), National Research Institute for Earth Science and Disaster Prevention (NEID), Geospatial Information Authority of Japan (GSI) and Japan Coast Guard (JCG) must be acknowledged. Offshore observations in the source area of the Tohoku-oki earthquake have been conducted for more than ten years under support of Ministry of Education, Culture, Sports, Science and Technology (MEXT), Japan. All the figures were made using GMT.

8.2.9 References

- Ammon, C.J., T. Lay, H. Kanamori, M. Cleveland, 2011. A rupture model of the 2011 off the Pacific coast of Tohoku Earthquake, *Earth Planets Space*, 63, 7, 693-696, doi:10.5047/eps.2011.05.015
- Altamimi, Z., X. Collilieux, J. Legrand, B. Garayt, and C. Boucher, 2007. ITRF2005: A new release of the International Terrestrial Reference Frame based on time series of station positions and Earth Orientation Parameters, *J. Geophys. Res.*, 112, B09401, doi:10.1029/2007JB004949
- Ando, R. and K. Imanishi, 2011. Possibility of M_W 9.0 mainshock triggered by diffusional propagation of after-slip from M_W 7.3 foreshock, *Earth Planets Space*, 63, 7, 767-771, doi:10.5047/eps.2011.05.016
- Asano, Y., T. Saito, Y. Ito, Y., K. Shiomi, H. Hirose, T. Matsumoto, S. Aoi, S. Hori, and S. Sekiguchi, 2011. Spatial distribution and focal mechanisms of aftershocks of the 2011 off the Pacific coast of Tohoku Earthquake, *Earth Planets Space*, 63, 7, 669-673, doi:10.5047/eps.2011.06.016
- Asano, K. and T. Iwata, 2012. Source model for strong ground motion generation in 0.1-10 Hz during the 2011 Tohoku earthquake, *Earth Planets Space*, 64, 12, 1111-1123, doi:10.5047/eps.2012.05.003
- Bilek, S.L., H. R. DeShon, and E. R. Engdahl, 2012. Spatial variations in earthquake source characteristics within the 2011 $M_W = 9.0$ Tohoku, Japan rupture zone, *Geophys. Res. Lett.*, 39, 9, L09304, doi:10.1029/2012GL051399
- Chiba, K., Y. Iio, and Y. Fukahata, 2012. Detailed stress fields in the focal region of the 2011 off the Pacific coast of Tohoku Earthquake—Implication for the distribution of moment release—, *Earth Planets Space*, 64, 12, 1157-1165, doi:10.5047/eps.2012.07.008
- Chu, R., S. Wei, D. V. Helmberger, Z. Zhan, L. Zhu, and H. Kanamori, 2011. Initiation of the great M_W 9.0 Tohoku-Oki earthquake, *Earth planet. Sci. Lett.*, 308, 3-4, 277-283, doi:10.1016/j.epsl.2011.06.031
- Diao, F., X. Xiong, R. Wang, Y. Zheng, T. R. Walter, H. Weng, and J. Li, 2014. Overlapping post-seismic deformation processes: afterslip and viscoelastic relaxation following the 2011 M_W 9.0 Tohoku (Japan) earthquake, *Geophys. J. Int.*, 196, 1, 218-229, doi:10.1093/gji/ggt376
- Duputel, Z., L. Rivera, H. Kanamori, G. P. Hayes, B. Hirshom, and S. Weinstein, 2011. Real-time W phase inversion during the 2011 off the Pacific coast of Tohoku earthquake, *Earth Planets Space*, 63, 7, 535-539, doi:10.5047/eps.2011.05.032
- Duputel, Z., V. C. Tsai, L. Rivera, H. Kanamori, 2013. Using centroid time-delays to characterize source durations and identify earthquakes with unique characteristics, *Earth planet. Sci. Lett.*, 374, 92-100, doi:10.1016/j.epsl.2013.05.024
- Frankel, A., 2013. Rupture History of the 2011 M 9 Tohoku Japan Earthquake Determined from Strong-Motion and High-Rate GPS Recordings: Subevents Radiating Energy in Different Frequency Bands, *Bull. seism. Soc. Am.*, 103, 2B, 1290-1306, doi:10.1785/0120120148
- Fujii, Y., K. Satake, S. Sakai, M. Shinohara, and T. Kanazawa, 2011. Tsunami source of the 2011 off the Pacific coast of Tohoku Earthquake, *Earth Planets Space*, 63, 7, 815-820, doi:10.5047/eps.2011.06.010
- Fujiwara, T., S. Kodaira, T. No, Y. Kaiho, N. Takahashi, and Y. Kaneda, 2011. The 2011 Tohoku-Oki

- Earthquake: Displacement Reaching the Trench Axis, *Science*, 334, 6060, 1240, doi:10.1126/science.1211554
- Fukahata, Y., Y. Yagi, and S. Miyazaki, 2012. Constraints on early stage rupture process of the 2011 Tohoku-oki earthquake from 1 Hz GPS data, *Earth Planets Space*, 64, 12, 1093-1099, doi:10.5047/eps.2012.09.007
- Fukuda, J., A. Kato, N. Kato, and Y. Aoki, 2013. Are the frictional properties of creeping faults persistent? Evidence from rapid afterslip following the 2011 Tohoku-oki earthquake, *Geophys. Res. Lett.*, 40, 14, 3613-3617, doi:10.1002/grl.50713
- Furumura, T., S. Takemura, S. Noguchi, T. Takemoto, T. Maeda, K. Iwai, and S. Padhy, 2011. Strong ground motions from the 2011 off-the Pacific-Coast-of-Tohoku, Japan ($M_W = 9.0$) earthquake obtained from a dense nationwide seismic network, *Landslides*, 8, 3, 333-338, doi:10.1007/s10346-011-0279-3
- Gamage, S. S. N., N. Umino, A. Hasegawa, and S. H. Kirby, 2009. Offshore double-planed shallow seismic zone in the NE Japan forearc region revealed by sP depth recorded by regional networks, *Geophys. J. Int.*, 78, 195–214, doi:10.1111/j.1365-246X.2009.04048.x
- Grilli, S. T, J. C. Harris, T. S. Tajalli Bakhsh, T. L. Masterlark, C. Kyriakopoulos, J. T. Kirby, and F. Shi, 2013. Numerical simulation of the 2011 Tohoku tsunami based on a new transient FEM co-seismic source: comparison to far- and near-field observations, *PAGEOPH*, 170, 1333-1359.
- Gusman, A. R., Y. Tanioka, S. Sakai, and H. Tsushima, 2012. Source model of the great 2011 Tohoku earthquake estimated from tsunami waveforms and crustal deformation data, *Earth planet. Sci. Lett.*, 341-344, 8, 234 - 242, doi:10.1016/j.epsl.2012.06.006
- Gusman, A. R., M. Fukuoka, Y. Tanioka, and S. Sakai, 2013. Effect of the largest foreshock (M_W 7.3) on triggering the 2011 Tohoku earthquake (M_W 9.0), *Geophys. Res. Lett.*, 40, 3, 497-500, doi:10.1002/grl.50153
- Harada, T., S. Murotani, and K. Satake, 2013. A deep outer-rise reverse-fault earthquake immediately triggered a shallow normal-fault earthquake: The 7 December 2012 off-Sanriku earthquake (M_W 7.3), *Geophys. Res. Lett.*, 40, 4214-4219, doi:10.1002/grl.50808
- Hardebeck, J. L., 2012. Coseismic and postseismic stress rotations due to great subduction zone earthquakes, *Geophys. Res. Lett.*, 39, 21, L21313, doi:10.1029/2012GL053438
- Hasegawa, A., N. Umino, and A. Takagi, 1978, Double-planed structure of the deep seismic zones in the northeastern Japan arc, *Tectonophysics*, 47, 43–58.
- Hasegawa, A., K. Yoshida, Okada, T., 2011. Nearly complete stress drop in the 2011 M_W 9.0 off the Pacific coast of Tohoku Earthquake, *Earth Planets Space*, 63, 7, 703-707, doi:10.5047/eps.2011.06.007
- Hasegawa, A., K. Yoshida, Y. Asano, T. Okada, T. Iinuma, and Y. Ito, 2012. Change in stress field after the 2011 great Tohoku-Oki earthquake, *Earth planet. Sci. Lett.*, 355-356, 11, 231 - 243, doi:10.1016/j.epsl.2012.08.042
- Hashimoto, C., A. Noda, T. Sagiya and M. Matsu'ura, 2009. Interplate seismogenic zones along the Kuril–Japan trench inferred from GPS data inversion, *Nature Geoscience*, 2, 141 – 144,

doi:10.1038/ngeo421

Hashimoto, C., A. Noda, and M. Matsu'ura, 2012. The M_W 9.0 northeast Japan earthquake: total rupture of a basement asperity, *Geophys. J. Int.*, 189, 1, 1-5, doi:10.1111/j.1365-246X.2011.05368.x

Hayashi, Y., H. Tsushima, K. Hirata, K. Kimura, and K. Maeda, 2011. Tsunami source area of the 2011 off the Pacific coast of Tohoku Earthquake determined from tsunami arrival times at offshore observation stations, *Earth Planets Space*, 63, 809-813.

Hayes, G. P., 2011. Rapid source characterization of the 2011 M_W 9.0 off the Pacific coast of Tohoku earthquake, *Earth Planets Space*, 63, 7, 529-534, doi:10.5047/eps.2011.05.012

Heki, K., S. Miyazaki and H. Tsuji, 1997, Silent fault slip following an interplate thrust earthquake at the Japan Trench, *Nature*, 386, 595-597.

Heki, K. and Y. Mitsui, 2013. Accelerated Pacific plate subduction following interplate thrust earthquakes at the Japan trench, *Earth planet. Sci. Lett.*, 363, 2, 44 - 49, doi:10.1016/j.epsl.2012.12.031

Hino, R., S. Ito, H. Shiobara, H. Shimamura, T. Sato, T. Kanazawa, J. Kasahara, and A. Hasegawa, 2000. Aftershock distribution of the 1994 Sanriku-oki earthquake (M_W 7.7) revealed by ocean bottom seismographic observation, *J. Geophys. Res.*, 105, 21697-21710.

Hino, R., Y. Yamamoto, A. Kuwano, M. Nishino, T. Kanazawa, T. Yamada, K. Nakahigashi, K. Mochizuki, M. Shinohara, K. Minato, G. Aoki, N. Okawara, M. Tanaka, M. Abe, E. Araki, S. Kodaira, G. Fujie, and Y. Kaneda, 2006. Hypocenter distribution of the main- and aftershocks of the 2005 Off Miyagi Prefecture earthquake located by ocean bottom seismographic data, *Earth Planets Space*, 58, 1543-1548.

Hino, R., R. Azuma, Y. Ito., Y. Yamamoto, K. Suzuki, H. Tsushima, S. Suzuki, M. Miyashita, T. Tomori, M. Arizono, and G. Tange, 2009. Insight into complex rupturing of the immature bending normal fault in the outer slope of the Japan Trench from aftershocks of the 2005 Sanriku earthquake ($M_W = 7.0$) located by ocean bottom seismometry, *Geochem Geophys Geosyst*, 10(7): Q07O18, doi:10.1029/2009GC002415

Hino, R., D. Inazu, Y. Ito, Y. Ohta, and T. Iinuma, 2013a. Ocean bottom pressure records of the 2011 Tohoku-Oki earthquake, *Proc. 11th SEGJ International Symposium*, 462-465, doi:10.1190/segj112013-117

Hino, R., D. Inazu, Y. Ohta, Y. Ito, S. Suzuki, T. Iinuma, Y. Osada, M. Kido, H. Fujimoto, Y. Kaneda, 2013b. Was the 2011 Tohoku-Oki earthquake preceded by aseismic preslip? Examination of seafloor vertical deformation data near the epicenter, *Mar Geophys Res.*, doi:10.1007/s11001-013-9208-2

Hirose, H., 2011. Tilt records prior to the 2011 off the Pacific coast of Tohoku Earthquake, *Earth Planets Space*, 63, 7, 655-658, doi:10.5047/eps.2011.05.009

Hirose, F., K. Miyaoka, N. Hayashimoto, T. Yamazaki, and M. Nakamura, 2011. Outline of the 2011 off the Pacific coast of Tohoku earthquake (M_W 9.0) -seismicity: Foreshocks, mainshock, aftershocks, and induced activity, *Earth Planets Space*, 63, 7, 513-518, doi:10.5047/eps.2011.05.019

Honda, R., Y. Yukutake, H. Ito, M. Harada, T. Aketagawa, A. Yoshida, S. Sakai, S. Nakagawa, N. Hirata, K. Obara, and H. Kimura, 2011. A complex rupture image of the 2011 off the Pacific coast of Tohoku

Earthquake revealed by the MeSO-net, *Earth Planets Space*, 63, 7, 583-588, doi:10.5047/eps.2011.05.034

Hooper, A., J. Pietrzak, W. Simons, H. Cui, R. Riva, M. Naeije, A. Terwisscha van Scheltinga, E. Schrama, G. Stelling, and A. Socquet, 2013. Importance of horizontal seafloor motion on tsunami height for the 2011 $M_W=9.0$ Tohoku-Oki earthquake, *Earth planet. Sci. Lett.*, 361, 469-479, doi:10.1016/j.epsl.2012.11.013

Hori, T. and S. Miyazaki, 2011. A possible mechanism of M 9 earthquake generation cycles in the area of repeating M 7 8 earthquakes surrounded by aseismic sliding, *Earth Planets Space*, 63, 773-777.

Hoshiya, M. and K. Iwakiri, 2011. Initial 30 seconds of the 2011 off the Pacific coast of Tohoku Earthquake ($M_W9.0$) - amplitude and θ_c for magnitude estimation for earthquake early Warning, *Earth Planets Space*, 63, 7, 553-557, doi:10.5047/eps.2011.06.015

Huang, Q. and X. Ding, 2012. Spatiotemporal Variations of Seismic Quiescence prior to the 2011 M 9.0 Tohoku Earthquake Revealed by an Improved Region-Time-Length Algorithm, *Bull. seism. Soc. Am.*, 102, 4, 1878-1883, doi:10.1785/0120110343

Ide, S., A. Baltay, and G. C. Beroza, 2011. Shallow dynamic overshoot and energetic deep rupture in the 2011 M_W 9.0 Tohoku-Oki earthquake, *Science*, 332, 6036, 1426-1429, doi:10.1126/science.1207020

Ide, S. and H. Aochi, 2013. Historical seismicity and dynamic rupture process of the 2011 Tohoku-Oki earthquake, *Tectonophysics*, 600, 1-13, doi:10.1016/j.tecto.2012.10.018

Igarashi, T., T. Matsuzawa, N. Umino, and A. Hasegawa, 2001. A. Spatial distribution of focal mechanisms for interplate and intraplate earthquakes associated with the subducting Pacific plate beneath the northeastern Japan arc: A triple-planed deep seismic zone, *J. Geophys. Res.*, 106, 2177-2191.

Iinuma, T., M. Ohzono, Y. Ohta, and S. Miura, 2011. Coseismic slip distribution of the 2011 off the Pacific coast of Tohoku Earthquake (M 9.0) estimated based on GPS data—Was the asperity in Miyagi-oki ruptured?, *Earth Planets Space*, 63, 643-648.

Iinuma, T., R. Hino, M. Kido, D. Inazu, Y. D. Osada, Y. Ito, M. Ohzono, H. Tsushima, S. Suzuki, H. Fujimoto, and S. Miura, 2012. Coseismic slip distribution of the 2011 off the Pacific Coast of Tohoku Earthquake ($M9.0$) refined by means of seafloor geodetic data, *J. geophys. Res.*, 117, B7, B07409, doi:10.1029/2012JB009186

Iinuma, T., R. Hino, M. Kido, Y. Osada, D. Inazu, Y. Ito, S. Suzuki, Y. Ohta, and H. Fujimoto, 2014. Investigation on the postseismic deformation associated with the 2011 Tohoku earthquake based on terrestrial and sea geodetic observations - to evaluate the further seismic hazard potential on the plate interface beneath the northeastern Japanese Islands, *proceedings IAG international symposium* (in press).

Imanishi, K., R. Ando, and Y. Kuwahara, 2012. Unusual shallow normal-faulting earthquake sequence in compressional northeast Japan activated after the 2011 off the Pacific coast of Tohoku earthquake, *Geophys. Res. Lett.*, 39, 9, L09306, doi:10.1029/2012GL051491

Ishii, M., 2011. High-frequency rupture properties of the M_W 9.0 off the Pacific coast of Tohoku Earthquake, *Earth Planets Space*, 63, 7, 609-614, doi:10.5047/eps.2011.07.009

- Ishibe, T., K. Shimazaki, K. Satake, and H. Tsuruoka, 2011. Change in seismicity beneath the Tokyo metropolitan area due to the 2011 off the Pacific coast of Tohoku Earthquake, *Earth Planets Space*, 63, 7, 731-735, doi:10.5047/eps.2011.06.001
- Ito, T., K. Ozawa, T. Watanabe, and T. Sagiya, 2011. Slip distribution of the 2011 off the Pacific coast of Tohoku Earthquake inferred from geodetic data, *Earth Planets Space*, 63, 7, 627-630, doi:10.5047/eps.2011.06.023
- Ito, Y., T. Tsuji, Y. Osada, M. Kido, D. Inazu, Y. Hayashi, H. Tsushima, R. Hino, and H. Fujimoto, 2011. Frontal wedge deformation near the source region of the 2011 Tohoku-Oki earthquake, *Geophys. Res. Lett.*, 38, 15, L00G05, doi:10.1029/2011GL048355
- Ito, Y., R. Hino, M. Kido, H. Fujimoto, Y. Osada, D. Inazu, Y. Ohta, T. Iinuma, M. Ohzono, S. Miura, M. Mishina, K. Suzuki, T. Tsuji, and J. Ashi, 2013. Episodic slow slip events in the Japan subduction zone before the 2011 Tohoku-Oki earthquake, *Tectonophysics*, 600, 14-26, doi:10.1016/j.tecto.2012.08.022
- Japan Coast Guard, 2012. Seafloor movements by seafloor geodetic observations before and after the 2011 off the Pacific coast of Tohoku earthquake. Report of the coordinating Committee for Earthquake Prediction, Japan 87, Chapter 3-7. Japan Coast Guard and Tohoku University, 2013. Seafloor movements observed by seafloor geodetic observations after the 2011 off the Pacific coast of Tohoku Earthquake, *Report of Coordinating Committee of Earthquake Prediction*, Vol. 90, 3-4, http://cais.gsi.go.jp/YOCHIREN/report/kaihou90/03_04.pdf
- Japan Metrological Agency, 2013. *Seismic activity in and around the Tohoku district (November 2012 - April 2013)*, Vol. 90, 3-41, http://cais.gsi.go.jp/YOCHIREN/report/kaihou90/03_01.pdf
- Johnson, K. M., J. Fukuda, and P. Segall, 2012. Challenging the rate-state asperity model: After-slip following the 2011 M9 Tohoku-oki, Japan, earthquake, *Geophys. Res. Lett.*, 39, 20, L20302, doi:10.1029/2012GL052901
- Kanamori, H., 1977, Seismic and aseismic slip along subduction zones and their tectonic implications, In: Talwani, M. Pitman, W.C. (Eds.), *Island Arcs, Deep Sea Trenches and Back-Arc Basins*, AGU, Washington, DC, pp.163-174, <http://dx.doi.org.10.1029/ME01p0163>
- Kato, N. and S. Yoshida, 2011. A shallow strong patch model for the 2011 great Tohoku-oki earthquake: A numerical simulation, *Geophys. Res. Lett.*, 38, doi:10.1029/2011GL048565
- Kato, A., S. Sakai, and K. Obara, 2011. A normal-faulting seismic sequence triggered by the 2011 off the Pacific coast of Tohoku Earthquake: Wholesale stress regime changes in the upper plate, *Earth Planets Space*, 63, 7, 745-748, doi:10.5047/eps.2011.06.014
- Kato, A. and T. Igarashi, 2012. Regional extent of the large coseismic slip zone of the 2011 M_W 9.0 Tohoku-Oki earthquake delineated by on-fault aftershocks, *Geophys. Res. Lett.*, 39, 15, L15301, doi:10.1029/2012GL052220
- Kato, A., K. Obara, T. Igarashi, H. Tsuruoka, S. Nakagawa, S. and N. Hirata, 2012. Propagation of Slow Slip Leading Up to the 2011 M_W 9.0 Tohoku-Oki Earthquake, *Science*, 335, 2, 705-708, doi:10.1126/science.1215141
- Kato, A., J. Fukuda, and K. Obara, 2013. Response of seismicity to static and dynamic stress changes

- induced by the 2011 $M_{9.0}$ Tohoku-Oki earthquake, *Geophys. Res. Lett.*, 40, 14, 3572-3578, doi:10.1002/grl.50699
- Katsumata, K., 2011. A long-term seismic quiescence started 23 years before the 2011 off the Pacific coast of Tohoku Earthquake ($M = 9.0$), *Earth Planets Space*, 63, 7, 709-712, doi:10.5047/eps.2011.06.033
- Kawamura, K., T. Sasaki, T. Kanamatsu, A. Sakaguchi, and Y. Ogawa, 2012. Large submarine landslides in the Japan Trench: A new scenario for additional tsunami generation, *Geophys. Res. Lett.*, 39, 5, L05308, doi:10.1029/2011GL050661
- Kawasaki, I., Y. Asai, Y. Tamura, T. Sagiya, N. Mikami, Y. Okada, M. Sakata and M. Kasahara, 1995. The 1992 Sanriku-Oki, Japan, Ultra-slow earthquake, *J. Phys. Earth*, 43, 105-116.
- Kawasaki, I., Y. Asai and Y. Tamura, 2001. Space-time distribution of interplate moment release including slow earthquakes and the seismo-geodetic coupling in the Sanriku-oki region along the Japan trench, *Tectonophysics*, 330, 267-283.
- Kido, M., Y. Osada, H. Fujimoto, R. Hino, and T. Ito, 2011. Trench-normal variation in observed seafloor displacements associated with the 2011 Tohoku-Oki earthquake, *Geophys. Res. Lett.*, 38, 24, L24303, doi:10.1029/2011GL050057
- Kido, M., H. Fujimoto, Y. Osada, Y. Ohta, J. Yamamoto, K. Tadokoro, T. Okuda, T. Watanabe, S. Nagai, and K. Yasuda, 2012. Development of GPS/A Seafloor Geodetic Network Along Japan Trench and Onset of Its Operation, Abstract T13F-2697 presented at 2012 Fall Meeting, AGU, San Francisco, Calif., 3-7 Dec.
- Kiser, E. and M. Ishii, 2012. The March 11, 2011 Tohoku-oki earthquake and cascading failure of the plate interface, *Geophys. Res. Lett.*, 39, L00G25, doi:10.1029/2012GL051170
- Kodaira, S., T. No, Y. Nakamura, T. Fujiwara, Y. Kaiho, S. Miura, N. Takahashi, Y. Kaneda, and A. Taira, 2012. Coseismic fault rupture at the trench axis during the 2011 Tohoku-oki earthquake, *Nature Geoscience*, 5(9), 646-650, doi:10.1038/ngeo1547
- Koper, K. D., A. R. Hutko, T. Lay, C. J. Ammon, and H. Kanamori, 2011a. Frequency-dependent rupture process of the 2011 M_W 9.0 Tohoku Earthquake: Comparison of short-period P wave backprojection images and broadband seismic rupture models, *Earth Planets Space*, 63, 7, 599-602, doi:10.5047/eps.2011.05.026
- Koper, K. D., A. R. Hutko, and T. Lay, 2011b. Along-dip variation of teleseismic short-period radiation from the 11 March 2011 Tohoku earthquake (M_W 9.0), *Geophys. Res. Lett.*, 38, 21, L21309, doi:10.1029/2011GL049689
- Koketsu, K., Y. Yokota, N. Nishimura, Y. Yagi, S. Miyazaki, K. Satake, Y. Fujii, H. Miyake, S. Sakai, Y. Yamanaka, and T. Okada, 2011. A unified source model for the 2011 Tohoku earthquake, *Earth planet. Sci. Lett.*, 310, 3-4, 480-487, doi:10.1016/j.epsl.2011.09.009
- Kosuga, M. and K. Watanabe, 2011. Seismic activity around the northern neighbor of the 2011 off the Pacific coast of Tohoku Earthquake with emphasis on a potentially large aftershock in the area, *Earth Planets Space*, 63, 719-723.

- Kubo, H. and Y. Kakehi, 2013. Source Process of the 2011 Tohoku Earthquake Estimated from the Joint Inversion of Teleseismic Body Waves and Geodetic Data Including Seafloor Observation Data: Source Model with Enhanced Reliability by Using Objectively Determined Inversion Settings, *Bull. seism. Soc. Am.*, 103, 2B, 1195-1220, doi:10.1785/0120120113
- Kubo, H., K. Asano, and T. Iwata, 2013. Source-rupture process of the 2011 Ibaraki-oki, Japan, earthquake (M_W 7.9) estimated from the joint inversion of strong-motion and GPS Data: Relationship with seamount and Philippine Sea Plate, *Geophys. Res. Lett.*, 40, 12, 3003-3007, doi:10.1002/grl.50558
- Kumagai, H., N. Pulido, E. Fukuyama, and S. Aoi, 2013. High-frequency source radiation during the 2011 Tohoku-Oki earthquake, Japan, inferred from KiK-net strong-motion seismograms, *J. geophys. Res.*, 118, 1, 222-239, doi:10.1029/2012JB009670
- Kurahashi, S. and K. Irikura, 2011. Source model for generating strong ground motions during the 2011 off the Pacific coast of Tohoku Earthquake, *Earth Planets Space*, 63, 7, 571-576, doi:10.5047/eps.2011.06.044
- Kurahashi, S. and K. Irikura, 2013. Short-Period Source Model of the 2011 M_W 9.0 Off the Pacific Coast of Tohoku Earthquake, *Bull. seism. Soc. Am.*, 103, 2B, 1373-1393, doi:10.1785/0120120157
- Lay, T., C. J. Ammon, H. Kanamori, L. Xue, and M. J. Kim, 2011a. Possible large near-trench slip during the 2011 M_W 9.0 off the Pacific coast of Tohoku earthquake, *Earth Planets Space*, 63, 7, 687-692, doi:10.5047/eps.2011.05.033
- Lay, T., C. J. Ammon, H. Kanamori, M. J. Kim, and L. Xue, 2011b. Outer trench-slope faulting and the 2011 M_W 9.0 off the Pacific coast of Tohoku Earthquake, *Earth Planets Space*, 63, 7, 713-718, doi:10.5047/eps.2011.05.006
- Lay, T., H. Kanamori, C. J. Ammon, K. D. Koper, A. R. Hutko, L. Ye, H. Yue, and T. M. Rushing, 2012. Depth-varying rupture properties of subduction zone megathrust faults, *J. geophys. Res.*, 117, B4, B04311, doi:10.1029/2011JB009133
- Lay, T., Z. Duputel, L. Ye, and H. Kanamori, 2013. The December 7, 2012 Japan Trench intraplate doublet (M_W 7.2, 7.1) and interactions between near-trench intraplate thrust and normal faulting, *Phys. Earth planet. Interiors*, 220, 73-78, doi:10.1016/j.pepi.2013.04.009
- Lee, S.-J., B.-S. Huang, M. Ando, H.-C. Chiu, and J.-H. Wang, 2011. Evidence of large scale repeating slip during the 2011 Tohoku-Oki earthquake, *Geophys. Res. Lett.*, 38, 19, L19306, doi:10.1029/2011GL049580
- Loveless, J. P. and B. J. Meade, 2010. Geodetic imaging of plate motions, slip rates, and partitioning of deformation in Japan, *J. Geophys. Res.*, 115, B02410, doi:10.1029/2008JB006248
- Loveless, J. P. and B. J. Meade, 2011. Spatial correlation of interseismic coupling and coseismic rupture extent of the 2011 $M_W = 9.0$ Tohoku-oki earthquake, *Geophys. Res. Lett.*, 38, 17, L17306, doi:10.1029/2011GL048561
- MacInnes B. T., A. R. Gusman, R. J. LeVeque, and Yuichiro Tanioka, 2013. Comparison of Earthquake Source Models for the 2011 Tohoku Event Using Tsunami Simulations and Near-Field Observations, *Bulletin of the Seismological Society of America*, 103:1256-1274; doi:10.1785/0120120121

- Maeda, T., T. Furumura, S. Sakai, and M. Shinohara, 2011. Significant tsunami observed at ocean-bottom pressure gauges during the 2011 off the Pacific coast of Tohoku Earthquake, *Earth Planets Space*, 63, 7, 803-808, doi:10.5047/eps.2011.06.005
- Marsan, D. and B. Enescu, 2012. Modeling the foreshock sequence prior to the 2011, M_W 9.0 Tohoku, Japan, earthquake, *J. geophys. Res.*, 117, B6, B06316, doi:10.1029/2011JB009039
- Matsuzawa T., N. Uchida, T. Igarashi, T. Okada, and A. Hasegawa, 2004. Repeating earthquakes and quasi-static slip on the plate boundary east off northern Honshu, Japan, *Earth Planets Space*, 56, 803-811.
- Meng, L., A. Inbal, and J.-P. Ampuero, 2011. A window into the complexity of the dynamic rupture of the 2011 M_W 9 Tohoku-Oki earthquake, *Geophys. Res. Lett.*, 38, L00G07, doi:10.1029/2011GL048118
- Minoura, K., Imamura, F., Sugawara, D., Kono, Y., Iwashita, T., 2001. The 869 Jogan tsunami deposit and recurrence interval of large-scale tsunami on the Pacific coast of northeast Japan, *Journal of Natural Disaster Science*, 23, 83-88.
- Mitsui, Y., N. Kato, Y. Fukahata, and K. Hirahara, 2012. Megaquake cycle at the Tohoku subduction zone with thermal fluid pressurization near the surface, *Earth and Planetary Science Letters*, 325-326, 21-26.
- Miyazaki, S., J. J. McGuire, and P. Segall, 2011. Seismic and aseismic fault slip before and during the 2011 off the Pacific coast of Tohoku Earthquake, *Earth Planets Space*, 63, 7, 637-642, doi:10.5047/eps.2011.07.001
- Miyazawa, M., 2011. Propagation of an earthquake triggering front from the 2011 Tohoku-Oki earthquake, *Geophys. Res. Lett.*, 38, 23, L23307, doi:10.1029/2011GL049795
- Miyazawa, M., 2012. Detection of seismic events triggered by P-waves from the 2011 Tohoku-Oki earthquake, *Earth Planets Space*, 64, 12, 1223-1229, doi:10.5047/eps.2012.07.003
- Mori, N., Takahashi, T., Yasuda, T. and Yanagisawa, H., 2011. Survey of 2011 Tohoku earthquake tsunami inundation and run-up, *Geophys. Res. Lett.*, 38, L00G14, doi:10.1029/2011GL049210
- Munekane, H., 2012. Coseismic and early postseismic slips associated with the 2011 off the Pacific coast of Tohoku Earthquake sequence: EOF analysis of GPS kinematic time series, *Earth Planets Space*, 64, 12, 1077-1091, doi:10.5047/eps.2012.07.009
- Nakahara, H., Sato, H., Nishimura, T. and Fujiwara, H., 2011. Direct observation of rupture propagation during the 2011 off the Pacific coast of Tohoku Earthquake (M_W 9.0) using a small seismic array, *Earth Planets Space*, 63, 7, 589-594, doi:10.5047/eps.2011.06.002
- Nakanishi, M. and E., L. Winterer, 1998. Tectonic history of the Pacific-Farallon-Phoenix triple junction from late Jurassic to early Cretaceous: An abandoned Mesozoic spreading system in the central Pacific Basin, *J. Geophys. Res.*, 103, 12453-12468.
- Nanjo, K. Z., N. Hirata, K. Obara, and K. Kasahara, 2012. Decade-scale decrease in b value prior to the M_9 -class 2011 Tohoku and 2004 Sumatra quakes, *Geophys. Res. Lett.*, 39, 20, L20304, doi:10.1029/2012GL052997

- Nettles, M., G. Ekström, and H. C. Koss, 2011. Centroid-moment-tensor analysis of the 2011 off the Pacific coast of Tohoku Earthquake and its larger foreshocks and aftershocks, *Earth Planets Space*, 63, 7, 519-523, doi:10.5047/eps.2011.06.009
- Nishimura, T., T. Hirasawa, S. Miyazaki, T. Sagiya, T. Tada, S. Miura, and K. Tanaka, 2004. Temporal change of interplate coupling in northeastern Japan during 1995 – 2002 estimated from continuous GPS observations, *Geophys J. Int.*, 157, 901-916
- Nishimura, T., Munekane, H. and Yarai, H., 2011. The 2011 off the Pacific coast of Tohoku Earthquake and its aftershocks observed by GEONET, *Earth Planets Space*, 63, 7, 631-636, doi:10.5047/eps.2011.06.025
- Obana, K., G. Fujie, T. Takahashi, Y. Yamamoto, Y. Nakamura, S. Kodaira, N. Takahashi, Y. Kaneda, and M. Shinohara, 2012. Normal-faulting earthquakes beneath the outer slope of the Japan Trench after the 2011 Tohoku earthquake: Implications for the stress regime in the incoming Pacific plate, *Geophysical Research Letters*, 39, 7, doi:10.1029/2011gl050399
- Obana K., S. Kodaira, M. Shinohara, R. Hino, K. Uehira, H. Shiobara, K. Nakahigashi, T. Yamada, H. Sugioka, A. Ito, Y. Nakamura, S. Miura, T. No, and N. Takahashi, 2013. Aftershocks near the updip end of the 2011 Tohoku-Oki earthquakes, *Earth Planet Sci Lett*, 382(0):111–116, doi:10.1016/j.epsl.2013.09.007
- Obana, K., S. Kodaira, Y. Nakamura, T. Sato, G. Fujie, T. Takahashi, and Yojiro Yamamoto, 2014. Aftershocks of the December 7, 2012 intraplate doublet near the Japan Trench axis, *Planets and Space 2014*, 66:24, <http://www.earth-planets-space.com/content/66/1/24>
- Ohta, Y., S. Miura, M. Ohzono, S. Kita, T. Iinuma, T. Demachi, K. Tachibana, T. Nakayama, S. Hirahara, S. Suzuki, T. Sato, N. Uchida, A. Hasegawa, and N. Umino, 2011. Large intraslab earthquake (2011 April 7, M 7.1) after the 2011 off the Pacific coast of Tohoku Earthquake (M 9.0): Coseismic fault model based on the dense GPS network data, *Earth Planets Space*, 63, 1207–1211
- Ohta, Y., R. Hino, D. Inazu, M. Ohzono, Y. Ito, M. Mishina, T. Iinuma, J. Nakajima, Y. Osada, K. Suzuki, H. Fujimoto, K. Tachibana, T. Demachi, S. Miura, 2012. Geodetic constraints on afterslip characteristics following the March 9, 2011, Sanriku-oki earthquake, Japan, *Geophys. Res. Lett.*, 39, L16304, doi:10.1029/2012GL052430
- Ohzono, M., Y. Yabe, T. Iinuma, Y. Ohta, S. Miura, K. Tachibana, T. Sato, and T. Demachi, 2012. Strain anomalies induced by the 2011 Tohoku Earthquake (M_W 9.0) as observed by a dense GPS network in northeastern Japan, *Earth Planets Space*, 64, 12, 1231-1238, doi:10.5047/eps.2012.05.015
- Okada, T., T. Yaginuma, N. Umino, T. Kono, T. Matsuzawa, S. Kita and A. Hasegawa, 2005, The 2005 $M7.2$ MIYAGI-OKI earthquake, NE Japan: Possible rerupturing of one of asperities that caused the previous $M7.4$ earthquake, doi:10.1029/2005GL024613
- Okada, T., K. Yoshida, S. Ueki, J. Nakajima, N. Uchida, T. Matsuzawa, N. Umino, N., and A. Hasegawa, 2011. Shallow inland earthquakes in NE Japan possibly triggered by the 2011 off the Pacific coast of Tohoku Earthquake, *Earth Planets Space*, 63, 7, 749-754, doi:10.5047/eps.2011.06.027
- Okal, E. A., 2013. From 3-Hz P Waves to 0S2: No Evidence of A Slow Component to the Source of the

- 2011 Tohoku Earthquake, *Pure appl. Geophys.*, 170, 6-8, 963-973, doi:10.1007/s00024-012-0500-x
- Ozawa, S., T. Nishimura, H. Suito, T. Kobayashi, M. Tobita, and T. Imakiire, 2011. Coseismic and postseismic slip of the 2011 magnitude-9 Tohoku-Oki earthquake, *Nature*, doi:10.1038/nature10227
- Ozawa, S., T. Nishimura, H. Munekane, H. Suito, T. Kobayashi, M. Tobita, and T. Imakiire, 2012. Preceding, coseismic, and postseismic slips of the 2011 Tohoku earthquake, Japan, *J. geophys. Res.*, 117, B7, B07404, doi:10.1029/2011JB009120
- Pacheco, J. F., L. R. Sykes, C. H. Scholz, 1993. Nature of seismic coupling along simple plate boundaries of the subduction type, *J. Geophys. Res.*, 98, 14133–14159, <http://dx.doi.org/10.1029/93JB00349>
- Peterson, E. T., T. Seno, 1984. Factors affecting seismic moment release rates in subduction zones, *J. Geophys. Res.*, 89, 10233–10248, <http://dx.doi.org/10.1029/JB089iB12p10233>
- Pollitz, F. F., R. Bürgmann, and P. Banerjee, 2011. Geodetic slip model of the 2011 $M9.0$ Tohoku earthquake, *Geophys. Res. Lett.*, 38, L00G08, doi:10.1029/2011GL048632
- Romano, F., A. Piatanesi, S. Lorito, N. D'Agostino, K. Hirata, S. Atzori, Y. Yamazaki, and M. Cocco, 2012. Clues from joint inversion of tsunami and geodetic data of the 2011 Tohoku-oki earthquake, *Sci. Rep.*, 2, 385, 1-8, doi:10.1038/srep00385
- Roten, D., H. Miyake, and K. Koketsu, 2012. A Rayleigh wave back-projection method applied to the 2011 Tohoku earthquake, *Geophys. Res. Lett.*, 39, 2, L02302, doi:10.1029/2011GL050183
- Ruff, L., and H. Kanamori, 1980. Seismicity and the subduction process, *Phys. Earth Planet. Inter.*, 23, 240-252.
- Saito, T., Y. Ito, D. Inazu, and R. Hino, 2011. Tsunami source of the 2011 Tohoku-Oki earthquake, Japan: Inversion analysis based on dispersive tsunami simulations, *Geophys. Res. Lett.*, 38, L00G19, doi:10.1029/2011GL049089
- Satake, K., Y. Fujii, T. Harada, and Y. Namegaya, 2013. Time and Space Distribution of Coseismic Slip of the 2011 Tohoku Earthquake as Inferred from Tsunami Waveform Data, *Bull. seism. Soc. Am.*, 103, 2B, 1473-1492, doi:10.1785/0120120122
- Satake, K. and Y. Fujii, 2014. Source Models of the 2011 Tohoku Earthquake and Long-Term Forecast of Large Earthquakes, *J. Disaster Res.*, 9 (in press).
- Sato, M., T. Ishikawa, N. Ujihara, S. Yoshida, M. Fujita, M. Mochizuki, and A. Asada, 2011. Displacement Above the Hypocenter of the 2011 Tohoku-Oki Earthquake, *Science*, 332, 6036, 1395, doi:10.1126/science.1207401
- Sato, T., S. Hiratsuka, and J. Mori, 2013. Precursory Seismic Activity Surrounding the High-Slip Patches of the 2011 M_W 9.0 Tohoku-Oki Earthquake, *Bull. seism. Soc. Am.*, 106, 6, 3104-3114, doi:10.1785/0120130042
- Sawai, Y., Y. Namegaya, Y. Okamura, K. Satake, and M. Shishikura, 2012. Challenges of anticipating the 2011 Tohoku earthquake and tsunami using coastal geology, *Geophys. Res. Lett.*, 39, 21, L21309, doi:10.1029/2012GL053692

- Scholz, C. H., 2002. *The Mechanics of Earthquakes and Faulting*, 471 pp, Cambridge Univ. Press, Cambridge.
- Seno, T., 1979. Intraplate seismicity in Tohoku and Hokkaido and large interplate earthquakes: a possibility of a large interplate earthquake off the southern Sanriku coast, northern Japan., *J. Phys. Earth*, 27, 21–51, <http://dx.doi.org/10.4294/jpe1952.27.21>
- Shao, G., X. Li, C. Ji, and T. Maeda, 2011. Focal mechanism and slip history of the 2011 M_W 9.1 off the Pacific coast of Tohoku earthquake, constrained with teleseismic body and surface waves, *Earth Planets Space*, 63, 7, 559-564, doi:10.5047/eps.2011.06.028
- Shibazaki, B., T. Matsuzawa, A. Tsutsumi, K. Ujiie, A. Hasegawa, and Y. Ito, 2011. 3D modeling of the cycle of a great Tohoku-oki earthquake, considering frictional behavior at low to high slip velocities, *Geophys. Res. Lett.*, 38, L21305, doi:10.1029/2011GL049308
- Shishikura, M., Y. Sawai, Y. Okamura, J. Komatsubara, T.-T. Aung, T. Ishiyama, O. Fujiwara, and S. Fujino, S., 2007. Age and distribution of tsunami deposit in the Ishinomaki plain, northeastern Japan. *Annual Report on Active Fault and Paleoequake Researches*, 7, 31–46.
- Shishikura, M., Y. Sawai, Y. Yukutani, and Y. Okamura, 2010. Simulation of the gigantic tsunami during Heian period — the 869 tsunami in Jogan era (in Japanese). *Active Fault and Earthquake Research Center News*, 16 August, 1–16.
- Simons, M., S. E. Minson, A. Sladen, F. Ortega, J. Jiang, S.E. Owen, L. Meng, J.-P. Ampuero, S. Wei, R. Chu, D. V. Helmberger, H. Kanamori, E. Hetland, A.W. Moore, and F. H. Webb, 2011. The 2011 magnitude 9.0 Tohoku-Oki earthquake: Mosaicking the megathrust from seconds to centuries, *Science*, 332, 6036, 1421-1425, doi:10.1126/science.1206731
- Strasser, M., M. Koelling, C. dos Santos Ferreira, H. G. Fink, T. Fujiwara, S. Henkel, K. Ikehara, T. Kanamatsu, K. Kawamura, S. Kodaira, M. Roemer and G. Wefer, R/V Sonne Cruise SO219A scientists, and JAMSTEC Cruise MR12-E01 scientists, 2013. A slump in the trench; tracking the impact of the 2011 Tohoku-Oki earthquake, *Geology*, 41, 935-938, doi:10.1130G34477.1
- Suito, H., T. Nishimura, M. Tobita, T. Imakiire, and S. Ozawa, 2011. Interplate fault slip along the Japan Trench before the occurrence of the 2011 off the Pacific coast of Tohoku Earthquake as inferred from GPS data, *Earth Planets Space*, 63, 7, 615-619, doi:10.5047/eps.2011.06.053
- Suwa, Y., S. Miura, A. Hasegawa, T. Sato and K. Tachibana, 2006, Interplate coupling beneath NE Japan inferred from three-dimensional displacement field, doi:10.1029/2004JB003203
- Suzuki, W., S. Aoi, H. Sekiguchi, and T. Kunugi, 2011. Rupture process of the 2011 Tohoku-Oki mega-thrust earthquake ($M9.0$) inverted from strong-motion data, *Geophys. Res. Lett.*, 38, L00G16, doi:10.1029/2011GL049136
- Suzuki, K., R. Hino, Y. Ito, Y. Yamamoto, S. Suzuki, H. Fujimoto, M. Shinohara, M. Abe, Y. Kawaharada, Y. Hasegawa, and Y. Kaneda, 2012. Seismicity near the hypocenter of the 2011 off the Pacific coast of Tohoku earthquake deduced by using ocean bottom seismographic data, *Earth Planets Space*, 64, 12, 1125-1135, doi:10.5047/eps.2012.04.010
- Takahashi, H., 2011. Static strain and stress changes in eastern Japan due to the 2011 off the Pa-

cific coast of Tohoku Earthquake, as derived from GPS data, *Earth Planets Space*, 63, 7, 741-744, doi:10.5047/eps.2011.06.049

Tajima, F. and B. L. N. Kennett, 2012. Interlocking of heterogeneous plate coupling and aftershock area expansion pattern for the 2011 Tohoku-Oki M_W 9 earthquake, *Geophys. Res. Lett.*, 39, 5, L05307, doi:10.1029/2011GL050703

Tanaka, S., 2012. Tidal triggering of earthquakes prior to the 2011 Tohoku-Oki earthquake (M_W 9.1), *Geophys. Res. Lett.*, 39, L00G26, doi:10.1029/2012GL051179

Tanioka, Y., and K. Satake, 1996a. Tsunami generation by horizontal displacement of ocean bottom, *Geophys. Res. Lett.* 23, 8, 861–864.

Tanioka, Y. and K. Satake, 1996b, Fault parameters of the 1896 Sanriku Tsunami Earthquake estimated from Tsunami Numerical Modeling, *Geophys. Res. Lett.*, 23, 1549–1552.

Tanioka, Y., and T. Seno, 2001. Sediment effect on tsunami generation of the 1896 Sanriku tsunami earthquake, *Geophys. Res. Lett.*, 28, 17, 3389–3392.

Terakawa T. and M. Matsu'ura, 2010. The 3-D tectonic stress fields in and around Japan inverted from centroid moment tensor data of seismic events, *Tectonics*, doi:10.1029/2009TC002626

Terakawa, T., C. Hashimoto, and M. Matsu'ura, 2013. Changes in seismic activity following the 2011 Tohoku-oki earthquake: Effects of pore fluid pressure, *Earth planet. Sci. Lett.*, 365, 3, 17 - 24, doi:10.1016/j.epsl.2013.01.017

Toda, S., J. Lin, and R. S. Stein, 2011a. Using the 2011 M_W 9.0 off the Pacific coast of Tohoku Earthquake to test the Coulomb stress triggering hypothesis and to calculate faults brought closer to failure, *Earth Planets Space*, 63, 7, 725-730, doi:10.5047/eps.2011.05.010

Toda, S., R. S. Stein, and J. Lin, 2011b. Widespread seismicity excitation throughout central Japan following the 2011 $M=9.0$ Tohoku earthquake and its interpretation by Coulomb stress transfer, *Geophys. Res. Lett.*, 38, L00G03, doi:10.1029/2011GL047834

Toda, S. and R. S. Stein, 2013. The 2011 $M=9.0$ Tohoku oki earthquake more than doubled the probability of large shocks beneath Tokyo, *Geophys. Res. Lett.*, 40, 11, 2562-2566, doi:10.1002/grl.50524

Toda, S. and H. Tsutsumi, 2013. Simultaneous reactivation of two, subparallel, inland normal faults during the M_W 6.6 11 April 2011 Iwaki earthquake triggered by the M_W 9.0 Tohoku-oki, Japan, earthquake, *Bull. Seism. Soc. Am.*, 103, 2B, 1584-1602, doi:10.1785/0120120281

Uchida, N, T. Matsuzawa, A. Hasegawa, and T. Igarashi, 2003. Interplate quasi-static slip off Sanriku, NE Japan, estimated from repeating earthquakes, *Geophys. Res. Lett.*, 30, doi:10.1029/2003GL017452

Uchida, N. and T. Matsuzawa, 2013. Pre- and postseismic slow slip surrounding the 2011 Tohoku-oki earthquake rupture, *Earth planet. Sci. Lett.*, 374, 81-91, doi:10.1016/j.epsl.2013.05.021

Uchide, T., 2013. High-speed rupture in the first 20 s of the 2011 Tohoku earthquake, Japan, *Geophys. Res. Lett.*, 40, 12, 2993-2997, doi:10.1002/grl.50634

Ueda, H., M. Ohtake, H. Sato, 2001. Afterslip of the plate interface following the 1978 Miyagi-Oki,

Japan, earthquake, as revealed from geodetic measurement data, *Tectonophysics*, 338, 45-57.

Umino, N., T. Kono, T. Okada, J. Nakajima, T. Matsuzawa, N. Uchida, A. Hasegawa, Y. Tamura, and G. Aoki, 2006, Revisiting the three M 7 Miyagi-oki earthquakes in the 1930s: possible seismogenic slip on asperities that were re-ruptured during the 1978 $M=7.4$ Miyagi-oki earthquake, *Earth Planets Space*, 58, 587-1592.

Wang, D. and J. Mori, 2011a. Rupture process of the 2011 off the Pacific coast of Tohoku Earthquake (M_W 9.0) as imaged with back-projection of teleseismic P-waves, *Earth Planets Space*, 63, 7, 603-607, doi:10.5047/eps.2011.05.029

Wang, D. and J. Mori, 2011b. Frequency-dependent energy radiation and fault coupling for the 2010 M_W 8.8 Maule, Chile, and 2011 M_W 9.0 Tohoku, Japan, earthquakes, *Geophys. Res. Lett.*, 38, 22, L22308, doi:10.1029/2011GL049652

Wang, K., Y. Hu, J. He, 2012, Deformation cycles of subduction earthquakes in a viscoelastic Earth, *Nature*, 484, 327-332.

Yagi, Y. and Y. Fukahata, 2011. Rupture process of the 2011 Tohoku-oki earthquake and absolute elastic strain release, *Geophys. Res. Lett.*, 38, 19, L19307, doi:10.1029/2011GL048701

Yamanaka, Y. and M. Kikuchi, 2004, Asperity map along the subduction zone in northeastern Japan inferred from regional seismic data, *J. Geophys. Res.*, 109, B07307, doi:10.1029/2003JB002683

Yao, H., P. M. Shearer, and P. Gerstoft, 2012. Subevent location and rupture imaging using iterative backprojection for the 2011 Tohoku M_W 9.0 earthquake, *Geophys. J. Int.*, 190, 2, 1152-1168, doi:10.1111/j.1365-246X.2012.05541.x

Ye, L., T. Lay, and H. Kanamori, 2013. Ground Shaking and Seismic Source Spectra for Large Earthquakes around the Megathrust Fault Offshore of Northeastern Honshu, Japan, *Bull. seism. Soc. Am.*, 103, 2B, 1221-1241, doi:10.1785/0120120115

Yokota, Y., K. Koketsu, Y. Fujii, K. Satake, S. Sakai, M. Shinohara, and T. Kanazawa, 2011. Joint inversion of strong motion, teleseismic, geodetic, and tsunami datasets for the rupture process of the 2011 Tohoku earthquake, *Geophys. Res. Lett.*, 38, L00G21, doi:10.1029/2011GL050098

Yoshida, K., K. Miyakoshi, and K. Irikura, 2011. Source process of the 2011 off the Pacific coast of Tohoku Earthquake inferred from waveform inversion with long-period strong-motion records, *Earth Planets Space*, 63, 577-582.

Yoshida, Y., H. Ueno, D. Muto, and S. Aoki, 2011. Source process of the 2011 off the Pacific coast of Tohoku Earthquake with the combination of teleseismic and strong motion data, *Earth Planets Space*, 63, 7, 565-569, doi:10.5047/eps.2011.05.011

Yoshida, K., A. Hasegawa, T. Okada, T., Iinuma, Y. Ito, and Y. Asano, 2012. Stress before and after the 2011 great Tohoku-oki earthquake and induced earthquakes in inland areas of eastern Japan, *Geophys. Res. Lett.*, 39, 3, L03302, doi:10.1029/2011GL049729

Yue, H. and T. Lay, 2011. Inversion of high-rate (1 sps) GPS data for rupture process of the 11 March 2011 Tohoku earthquake (M_W 9.1), *Geophys. Res. Lett.*, 38, L00G09, doi:10.1029/2011GL048700

Yue, H. and T. Lay, 2013. Source Rupture Models for the M_W 9.0 2011 Tohoku Earthquake from Joint Inversions of High-Rate Geodetic and Seismic Data, *Bull. seism. Soc. Am.*, 103, 1242-1255, doi:10.1785/0120120119

Yukutake, Y., R. Honda, M. Harada, T. Aketagawa, H. Ito, and A. Yoshida, 2011. Remotely-triggered seismicity in the Hakone volcano following the 2011 off the Pacific coast of Tohoku Earthquake, *Earth Planets Space*, 63, 737-740.

Zhang, H., Z. Ge, and L. Ding, 2011. Three sub-events composing the 2011 off the Pacific coast of Tohoku Earthquake (M_W 9.0) inferred from rupture imaging by back-projecting teleseismic P waves, *Earth Planets Space*, 63, 7, 595-598, doi:10.5047/eps.2011.06.021